Follicular regulatory T cells control humoral autoimmunity via NFAT2-regulated CXCR5 expression

Vaeth, M. and Mueller, G. and Stauss, D. and Dietz, L. and Klein-Hessling, S. and Serfling, E. and Lipp, M. and Berberich, I. and Berberich-Siebelt, F.

This is a copy of the final article, which was first published online on 03 March 2014 and in final edited form in:

The Journal of Experimental Medicine
2014 MAR 10 ; 211(3): 545-561
doi: 10.1084/jem.20130604

Publisher: Rockefeller University Press

Published March 3, 2014

Follicular regulatory T cells control humoral autoimmunity via NFAT2-regulated CXCR5 expression

Martin Vaeth,[1] Gerd Müller,[2] Dennis Stauss,[2] Lena Dietz,[1] Stefan Klein-Hessling,[1] Edgar Serfling,[1] Martin Lipp,[2] Ingolf Berberich,[3] and Friederike Berberich-Siebelt[1,4]

[1]Department of Molecular Pathology, Institute of Pathology and [4]Comprehensive Cancer Center Mainfranken, Julius-Maximilians-University of Wuerzburg, 97080 Wuerzburg, Germany
[2]Department of Tumor Genetics and Immunogenetics, Max-Delbruck-Center for Molecular Medicine (MDC), 13092 Berlin, Germany
[3]Institute for Virology and Immunobiology, University of Wuerzburg, 97078 Wuerzburg, Germany

Maturation of high-affinity B lymphocytes is precisely controlled during the germinal center reaction. This is dependent on CD4$^+$CXCR5$^+$ follicular helper T cells (T_{FH}) and inhibited by CD4$^+$CXCR5$^+$Foxp3$^+$ follicular regulatory T cells (T_{FR}). Because NFAT2 was found to be highly expressed and activated in follicular T cells, we addressed its function herein. Unexpectedly, ablation of NFAT2 in T cells caused an augmented GC reaction upon immunization. Consistently, however, T_{FR} cells were clearly reduced in the follicular T cell population due to impaired homing to B cell follicles. This was T_{FR}-intrinsic because only in these cells NFAT2 was essential to up-regulate CXCR5. The physiological relevance for humoral (auto-)immunity was corroborated by exacerbated lupuslike disease in the presence of NFAT2-deficient T_{FR} cells.

CORRESPONDENCE
Friederike Berberich-Siebelt:
path230@mail.uni-wuerzburg.de

Abbreviations used: Blimp, B lymphocyte–induced maturation protein; Foxp3, Fork head box P3; GC, germinal center; nT_{reg}, thymus-derived natural Foxp3$^+$ regulatory T cell; PC, plasma cell; SLE, systemic lupus erythematosus; T_{conv}, conventional CD4$^+$ T cell; T_{FH}, follicular helper T cell; T_{FR}, follicular regulatory T cell.

The humoral arm of the immune response is a crucial element of adaptive immunity that involves antibody (Ab) production by plasma cells (PCs). PCs differentiate from B cells when activated in a T cell–dependent or –independent manner. T cell–dependent B cell activation is a tightly regulated process that includes germinal center (GC) formation, in which affinity maturation through somatic hypermutation, isotype switching, and the generation of memory cells take place. Dysregulation of the GC reaction can lead either to humoral immunodeficiency or to severe autoimmune disorders. Indeed, patients suffering from systemic lupus erythematosus (SLE), a potentially fatal autoimmune disease, show augmented GC formation leading to the production of auto-Abs attacking various tissues.

The GC reaction is conducted by highly specialized CD4$^+$ T lymphocytes called follicular T helper (T_{FH}) cells (Crotty, 2011). They provide cognate help to GC–B cells (Crotty, 2011). T_{FH} cells depend on the expression of the chemokine receptor CXCR5 and down-regulation of the chemokine receptor CCR7 to facilitate repositioning from T cell zones into B cell follicles, directly promoting GC immune responses (Ma et al., 2012). CXCR5 (CD185 or Burkitt lymphoma receptor 1) is a G protein–coupled seven transmembrane receptor for chemokine CXCL13, which is strongly expressed in the follicles of the spleen, lymph nodes, and Peyer's patches. Besides CXCR5, T_{FH} cells are characterized by the expression of various surface molecules, such as ICOS, CD40L, PD-1, and BTLA, and the massive production of IL-21 (Chtanova et al., 2004; Rasheed et al., 2006).

The differentiation into Th subtypes like Th1, Th2, Th9, and Th17 is directed by signature transcription factors. Accordingly, T_{FH} cells representing a distinct subset are reliant on a specific transcription factor, namely B cell lymphoma-6

M. Vaeth's present address is Dept. of Pathology and Cancer Institute, New York University School of Medicine, New York, NY.

The Rockefeller University Press $30.00
J. Exp. Med. 2014 Vol. 211 No. 3 545-561
www.jem.org/cgi/doi/10.1084/jem.20130604

Supplemental Material can be found at:
http://jem.rupress.org/content/suppl/2014/02/28/jem.20130604.DC1.html

Published March 3, 2014

(Bcl-6; Johnston et al., 2009; Yu et al., 2009; Kroenke et al., 2012). Importantly, Bcl-6 not only inhibits key transcription factors for Th1 and Th17, namely *Tbx21* and *Rorc* expression (Yu et al., 2009), but also represses B lymphocyte-induced maturation protein (Blimp-1), which attenuates the development of T_{FH} cells and subsequently GC responses (Johnston et al., 2009). Ectopic overexpression of Bcl-6 leads to the expression of CXCR5, although Bcl6 has not been demonstrated to transactivate *Cxcr5* or *Il21* directly (Yu et al., 2009; Kroenke et al., 2012). Because deletion of c-Maf, BATF, or IRF4 almost completely abrogated T_{FH} cell generation (Bauquet et al., 2009; Kwon et al., 2009; Ise et al., 2011; Bollig et al., 2012), the involvement and interrelation with other transcriptional regulators is likely. As the transcription of nuclear factor of activated T cells (NFAT) is strongly enhanced in T_{FH} cells (Rasheed et al., 2006) and NFAT cooperates with c-Maf and IRF4 (Ho et al., 1996; Rengarajan et al., 2002a; Farrow et al., 2011), NFAT proteins could be likewise involved.

The family of NFAT transcription factors consists of four Ca^{2+}-responsive members, known as NFAT1/NFATc2, NFAT2/NFATc1, NFAT3/NFATc4, and NFAT4/NFATc3 (Serfling et al., 2000; Müller and Rao, 2010). Upon TCR initiated Ca^{2+} influx and the subsequent activation of calmodulin/calcineurin, preformed NFAT1/NFAT4 are dephosphorylated and translocated into the nucleus, where they bind to GGA motifs (usually those with 3′-adenine tracts). Although most NFAT factors, including the long isoforms of NFAT2, are constitutively expressed, the shortest isoform of NFAT2, i.e., NFAT2/αA, is induced in effector cells through an autoregulatory mechanism that involves NFAT binding to the *Nfat2* P1 promoter (Chuvpilo et al., 2002; Serfling et al., 2012). Despite functional redundancies among individual NFAT members, which can consequently lead to a more severe impairment when two NFAT proteins are deleted (Peng et al., 2001; Rengarajan et al., 2002b; Vaeth et al., 2012), individual NFAT members also serve distinct roles. Therefore, single NFAT-deficient mice as well as exogenously expressed members or even their individual isoforms display divergent phenotypes (Nayak et al., 2009; Müller and Rao, 2010; Serfling et al., 2012).

As a precisely controlled process, the GC reaction involves various regulatory cell types. Notably, impaired function of thymus-derived natural $Foxp3^+$ (nT_{reg}) T cells (Sakaguchi et al., 2008) escalates GC responses, leading to the production of pathogenic auto-Abs and SLE in patients (Valencia et al., 2007; Bonelli et al., 2008, 2010). Accordingly, a special subset of nT_{reg} cells that share characteristics with T_{FH} cells, follicular regulatory T (T_{FR}) cells, was identified in GCs (Chung et al., 2011; Linterman et al., 2011; Wollenberg et al., 2011). Similar to T_{FH} cells, T_{FR} cells express CXCR5, ICOS, and PD-1, but in addition, they exhibit typical T_{reg} markers, such as Foxp3, CD25, GITR, and CTLA4 (Chung et al., 2011; Linterman et al., 2011; Wollenberg et al., 2011). Furthermore, T_{FR} cells not only express Bcl-6, but also high levels of Blimp-1, a known Foxp3 target gene (Zheng et al., 2007; Johnston et al., 2009; Linterman et al., 2011). They limit the magnitude of the GC reaction, i.e., the number of GC-B cells and the quantity and quality of secreted immunoglobulins, by direct repression of B cells (Lim et al., 2005; Wollenberg et al., 2011; Sage et al., 2013).

$Foxp3^+$ nT_{reg} cells localize to diverse tissues by the expression of the relevant homing receptors and suppress various cell types to avoid autoimmunity. To do so they adapt to part of the transcriptional program of the very cells they suppress (Josefowicz et al., 2012). Accordingly, T_{FR} cells express Bcl-6, which is required for CXCR5 expression (Johnston et al., 2009; Yu et al., 2009; Kroenke et al., 2012). However, as mentioned, Bcl-6 alone is not sufficient for CXCR5 expression, suggesting that additional transcription factors are involved in this process. NFAT2, highly expressed in both T_{FH} and GC-B cells, seemed like an unlikely candidate because we had found that NFAT2-deficient nT_{reg} cells not only express Foxp3 normally but are also fully suppressive (Vaeth et al., 2012). Nevertheless, when we studied the impact of T cell– or even T_{reg}-specific ablation of NFAT2, we observed an increased and pathogenic GC reaction, which was dominated by the altered homing behavior of NFAT2-deficient T_{FR} cells into B cell follicles. This could be attributed to the absolute dependence on NFAT2 for CXCR5 expression in T_{FR} cells being T_{FR}-specific and intrinsic. Therefore, a subset of T_{reg} cells, namely that of T_{FR} cells, does depend on a single member of NFAT, not for their general suppressor function, which is very much in line with our former data (Vaeth et al., 2012), but for proper tissue localization. This is of significance to disease because NFAT2-deficient T_{FR} cells failed to control humoral autoimmunity, as demonstrated in a model of murine SLE.

RESULTS

NFAT2 is strongly expressed and activated in follicular T cells

Because we had observed that NFAT2 has especially high expression in human T_{FH} cells (Rasheed et al., 2006), we addressed the expression of NFAT transcription factors in their murine counterparts. Microarray experiments revealed enhanced RNA expression of NFAT1 in $CD4^+ICOS^{hi}CXCR5^{hi}$ T_{FH} compared with activated $CD4^+ICOS^{hi}CXCR5^-$ T cells and/or $CD4^+ICOS^-CXCR5^-$ naive conventional T (T_{conv}) cells, but the family member most clearly up-regulated was NFAT2 (Fig. 1 A). Alternate definition of T_{FH} cells by $CD4^+PD\text{-}1^{hi}CXCR5^{hi}$ in comparison to $CD4^+PD\text{-}1^-CXCR5^-$ T_{conv} cells revealed the same dominance of NFAT2 by qRT-PCR, which was primarily caused by high *Nfat2 P1* promoter activity (Fig. 1 B). More importantly, the *P1* promoter was also more effective in $CD4^+PD\text{-}1^{hi}CXCR5^{hi}$ T_{FH} cells than in activated $CD4^+ICOS^{hi}$ T_{conv} cells (Fig. 1 B, lower graphs). Making use of BAC-transgenic *Nfatc1/egfp* reporter mice (Bhattacharyya et al., 2011; Hock et al., 2013), T_{FH} cells (defined as $CD4^+PD\text{-}1^{hi}CXCR5^{hi}$ or $CD4^+ICOS^{hi}CXCR5^{hi}$) from KLH- or SRBC-immunized mice exhibited the highest green fluorescence (Fig. 1 C and not depicted). This was reflected by the strong nuclear appearance of NFAT2, similar to that found in activated T_{conv} cells (Fig. 1 D). Corresponding to

Published March 3, 2014

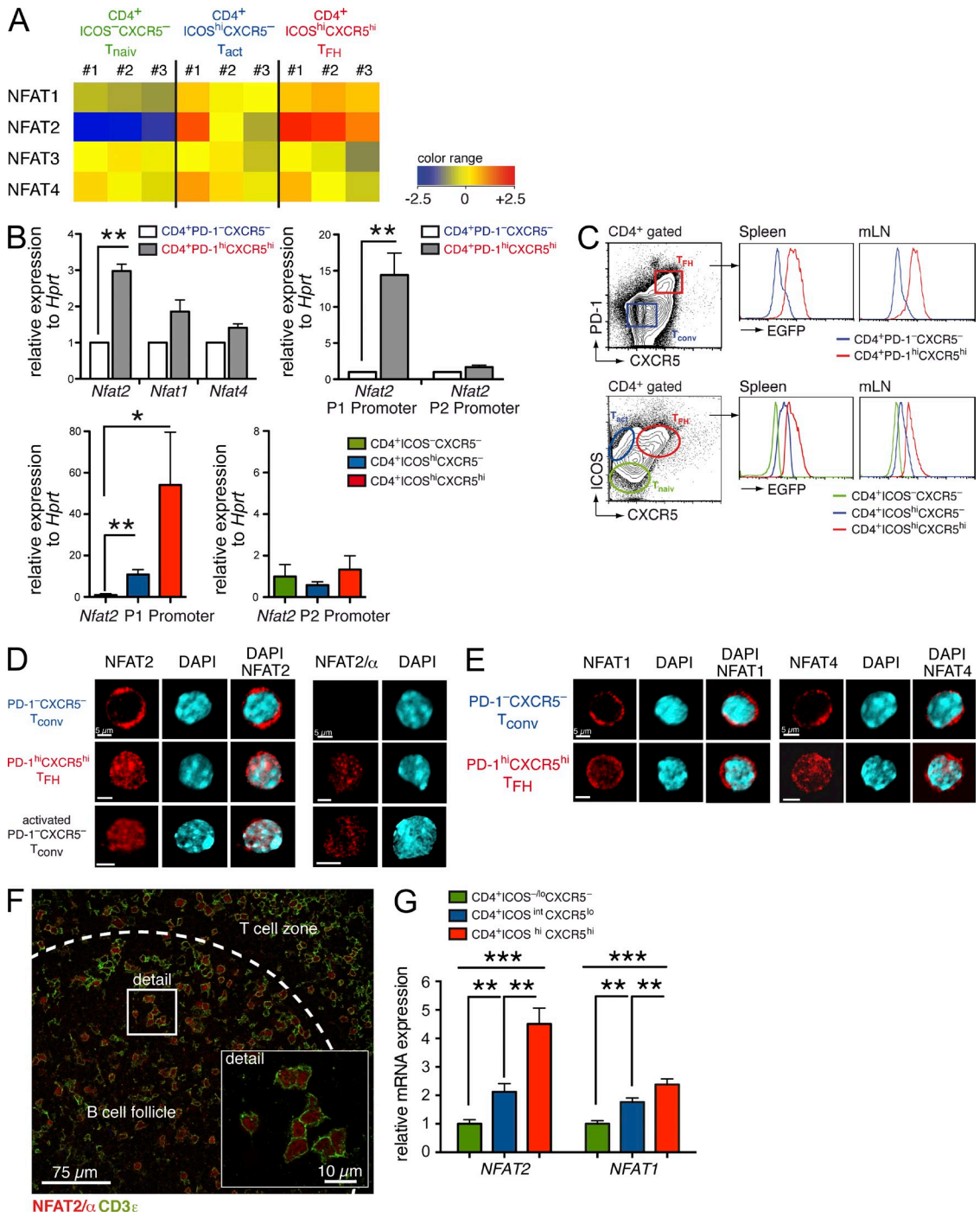

Figure 1. Expression and activation of NFAT2 in follicular T cells. (A) Microarray analysis of *Nfat* expression in FACS-sorted CXCR5^{-}ICOS^{-} (T_{naiv}), CXCR5^{-}ICOS^{hi} (T_{act}), and CXCR5^{hi}ICOS^{hi} (T_{FH}) CD4^{+} T cells of KLH-immunized mice; 3 independent experiments with 12 mice per group. (B, top) qRT-PCR for *Nfat2*, *Nfat1*, *Nfat4*, and *Nfat2* promoter *P1* (exon 1 to exon 3) and *P2* (exon 2 to exon 3) expression in CXCR5^{-}PD-1^{-} (T_{conv}) and CXCR5^{hi}PD-1^{hi} (T_{FH}) CD4^{+} T cells of KLH-immunized mice. (bottom) qRT-PCR for *Nfat2* promoter *P1* and *P2* expression of T cells sorted as in A from SRBC-immunized mice. (C) Flow cytometry of NFAT2 expression in CXCR5^{-}PD-1^{-} (T_{conv}), CXCR5^{hi}PD-1^{hi} (T_{FH}), CXCR5^{-}ICOS^{-} (T_{naiv}), CXCR5^{-}ICOS^{hi} (T_{act}), and CXCR5^{hi}ICOS^{hi} (T_{FH}) CD4^{+} T cells using KLH-immunized *Nfatc1/egfp* BAC-tg reporter mice. (D) Confocal microscopy of NFAT2 and NFAT2/α nuclear localization in FACS-sorted CXCR5^{-}PD-1^{-} (T_{conv}), with or without activation overnight by anti-CD3/28, and CXCR5^{hi}PD-1^{hi} (T_{FH}) CD4^{+} T cells from KLH-immunized mice. (E) Confocal microscopy of NFAT1 and NFAT4 nuclear localization in FACS-sorted CXCR5^{-}PD-1^{-} (T_{conv}) and CXCR5^{hi}PD-1^{hi} (T_{FH}) CD4^{+} T cells from KLH-immunized mice. (F) Histological analysis of NFAT2/α expression in follicular T cells of a chronically inflamed human tonsil (T cell zone = enriched for T cells; B cell follicle = fewer T cells; mantle zone = appearing dark due to no T cells). (G) Evaluation of *NFAT2* RNA expression in human CXCR5^{hi}ICOS^{hi} (T_{FH}) compared with CXCR5^{-}ICOS$^{-/lo}$ (T_{naiv}) and CXCR5^{lo}ICOS^{int} (T_{act}) CD4^{+} T cells, sorted from inflamed tonsils and analyzed by microarrays (three independent chip analyses per CD4^{+} T cell population, with each chip representing at least 3 donors; Rasheed et al., 2006). Values were normalized to T_{naiv} for NFAT 1 and NFAT2, respectively. (B and G) Student's *t* test: *, $P < 0.05$; **, $P < 0.005$; ***, $P < 0.001$.

Published March 3, 2014

the robust *Nfat2 P1* activity, NFAT2/α isoforms were dominantly expressed and activated in T_{FH} like in T_{conv} cells. NFAT1 and NFAT4 were also found to be activated in $CD4^+PD\text{-}1^{hi}CXCR5^{hi}$ cells, but to a lesser extent (Fig. 1 E). Prominent NFAT2 and especially NFAT2/α expression was verified in human T_{FH} cells in chronically inflamed tonsils (Fig. 1, F and G), conclusively confirming NFAT2 as robustly expressed and activated in human T_{FH} cells (Rasheed et al., 2006).

NFAT2 deficiency in T cells causes an augmented GC reaction

Next, we tested the consequence of T cell–specific NFAT2 ablation for the GC reaction *Nfat2$^{fl/fl}$ x Cd4cre* mice are healthy and show a fairly normal composition of lymphoid compartments (Vaeth et al., 2012). Nonetheless, we detected modest but considerably increased frequencies of T_{FH} cells in spleen and mesenteric LNs (mLNs) from NP-KLH–immunized *Nfat2$^{fl/fl}$ x Cd4cre* mice compared with *Cd4cre* littermates being significant over the complete distribution of the datasets (Fig. 2, A and B). By PNA staining of histological sections, however, we observed an even more clearly pronounced GC response (Fig. 2 C and not depicted). Flow cytometry reinforced a boosted frequency of $B220^+GL\text{-}7^+Fas^+$ GC-B cells in NP-KLH– or SRBCs-immunized *Nfat2$^{fl/fl}$ x Cd4cre* mice (Fig. 2 D and not depicted). Consecutively, the titer of the NP-specific Abs IgM and class-switched IgG1 and IgG3 was increased in *Nfat2$^{fl/fl}$ x Cd4cre* mice upon NP-KLH immunization (Fig. 2 E), revealing an overall amplification of the GC reaction upon loss of NFAT2 in T cells.

There are fewer Foxp3$^+$ T_{FR} cells among NFAT2-deficient CXCR5^{hi} follicular T cells

To unravel the increase in GC reaction in *Nfat2$^{fl/fl}$ x Cd4cre* mice at the molecular level, we performed global transcription analyses of FACS sorted $ICOS^{hi}CXCR5^{hi}$ T_{FH} cells in comparison to activated ($ICOS^{hi}CXCR5^-$) and naive ($ICOS^-CXCR5^-$) T_{conv} cells. In line with highest expression of NFAT2 in T_{FH} cells, NFAT2-deficient T_{FH} cells showed prevalence in the number of differently regulated transcripts (Fig. 3, A and B). We analyzed affected transcripts and found that T_{reg}-specific or –associated genes (Hill et al., 2007) were a self-contained group being reduced in *Nfat2$^{fl/fl}$ x Cd4cre* mice (Fig. 3 C). Performing quantitative RT-PCR from NFAT2-sufficient and NFAT2-deficient T_{FH} in comparison to T_{conv} cells again demonstrated a clear transcriptional decline of two tested key molecules for T_{FR}, namely Foxp3 and Blimp-1, whereas Bcl-6 was slightly increased, if quantities changed at all (Fig. 3 D). The additional loss of NFAT1 in follicular T cells had no major impact, suggesting NFAT2 as the prominent NFAT family member in T_{FR} cells (Fig. 3 D).

T cell–specific NFAT2 deficiency results in fewer T_{FR} cells within B cell follicles

Because microarray analyses of $CD4^+ICOS^{hi}CXCR5^{hi}$ T_{FH} cells revealed a reduction in the T_{reg} cell signature (Hill et al., 2007) upon NFAT2 deficiency, we tested the frequency of Foxp3$^+$ T_{reg} cells in the population of T_{conv} versus T_{FH} cells upon immunization. As NFAT2-sufficient and -deficient T_{conv} cells displayed the same number of Foxp3$^+$ T_{reg} cells, significantly fewer Foxp3$^+$ T_{FR} cells were detected among $PD\text{-}1^+CXCR5^+$ T_{FH} cells in mice lacking NFAT2 (Fig. 4 A). This was true irrespective of the kind and strength of immunization, shown by immunization with NP-KLH or SRBCs as well as by Ova in *Nfat2$^{fl/fl}$ x Cd4cre x* OT-II mice tested by flow cytometry and, in individual follicles, by immunohistochemistry (Fig. 4, A–D; and not depicted). Confocal microscopy discovered reduced numbers of Foxp3$^+$ T_{FR} cells within PNA-positive GC-areas in *Nfat2$^{fl/fl}$ x Cd4cre* mice (Fig. 4 E). For comparison, we addressed the impact of NFAT1 on T_{FR} cells. The numbers of T_{FR} cells in B cell follicles of immunized *Nfat1$^{-/-}$* mice were found unaltered, whereas additional NFAT1 deficiency in *Nfat2$^{fl/fl}$ x Cd4cre* mice might further impair the frequency of T_{FR} cells (Fig. 4, F and G). In summary, this defines NFAT2 as an important transcription factor for one specific subtype of nT_{reg} cells, namely T_{FR} cells, which are distributed mainly between B cells in GCs (unpublished data).

Impaired numbers of Foxp3$^+$ T_{FR} cells in B cell follicles is a NFAT2-regulated T_{reg}-intrinsic effect

Earlier we demonstrated that the generation of thymus-derived nT_{reg} cells, to which T_{FR} belong (Linterman et al., 2011), does not depend on NFAT1 and NFAT2 in terms of Foxp3 expression (Vaeth et al., 2012). This was not consistent with the observed decrease of Foxp3$^+$ cells within NFAT2-deficient $CXCR5^{hi}$ T_{FH} cell population. We therefore asked if the loss of Foxp3$^+$ cells was T_{reg}-intrinsic by crossing *Nfat2$^{fl/fl}$* mice to *Foxp3-IRES-Cre* (*FIC*; Wing et al., 2008) mice and found, again, a profound reduction of $CXCR5^{hi}$ T_{FR} cells upon immunization (Fig. 5 A). In line with our former findings, no alteration of nT_{reg} cell frequencies within the $CD4^+CXCR5^-PD\text{-}1^-$ T_{conv} population could be observed (Fig. 5 A). Immunohistochemistry confirmed fewer Foxp3$^+$ T_{FR} cells in reactive B cell follicles (Fig. 5 B). Comparable to the eradication of NFAT2 in all T cells, T_{reg}-specific NFAT2 deletion led to an augmented GC reaction (Fig. 5 C and not depicted) paralleled by an increase in antigen-specific IgM and IgG after immunization (Fig. 5 D). To exclude secondary effects caused by the influence of other cells, e.g., via IL-2 production, we adoptively co-transferred WT and NFAT2-deficient $CD4^+$ T cells at a ratio of 1:1 into *Rag1$^{-/-}$* mice, followed by immunization (Fig. 5 E). WT T cells were distinguished by CD90.1 from $CD90.2^+$ *Nfat2$^{-/-}$* T cells. Again, we found a decrease in T_{FR} cells specifically within the $CD90.2^+$ NFAT2-deficient T cell population (Fig. 5 E). The phenotype achieved by T cell–specific loss of NFAT2 for the GC reaction was similar to a total depletion of T_{reg} cells. This was performed by injection of diphtheria toxin into immunized $Foxp3^{DTR\text{-}eGFP}$ mice (Lahl et al., 2007). Clearly reduced numbers of T_{FR} cells were seconded by an expansion of GCs upon depletion of T_{reg} cells (Fig. 5 F and not depicted). Overall, these data account for an NFAT2-dependent and T_{FR} cell–intrinsic effect to limit humoral immune reaction.

Published March 3, 2014

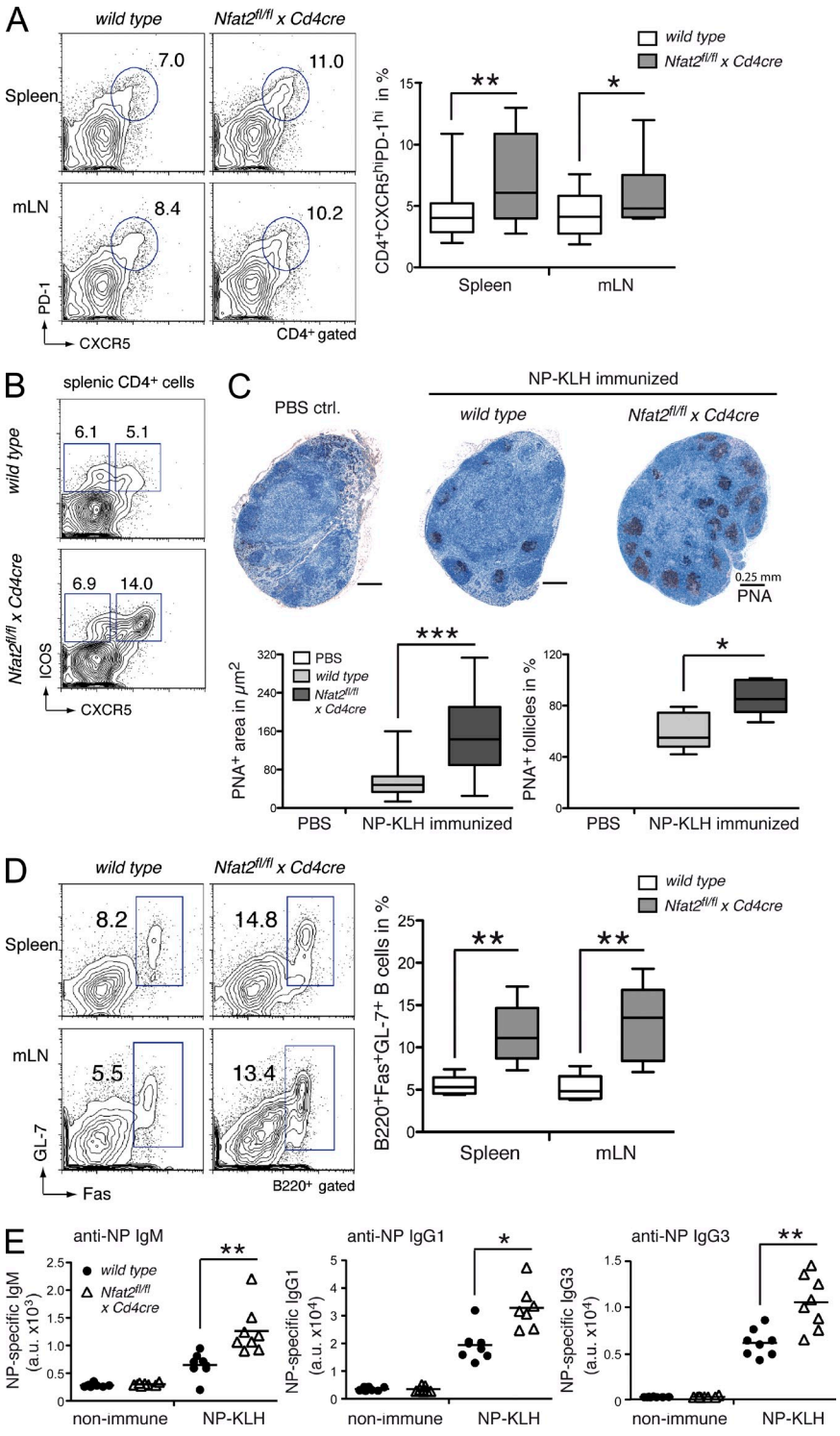

Figure 2. NFAT2 deficiency in T cells causes augmented GC reaction upon immunization. (A) Representative flow cytometry of splenic $CD4^+CXCR5^{hi}PD\text{-}1^{hi}$ T_{FH} cells from WT and *Nfat2*$^{fl/fl}$ *x Cd4cre* mice 10 d after KLH immunization (left), plus compilation of 12 independent experiments (right). (B) Analysis of splenic $CD4^+CXCR5\text{-}ICOS^{hi}$ (T_{act}) and $CD4^+CXCR5^{hi}ICOS^{hi}$ (T_{FH}) population of WT and *Nfat2*$^{fl/fl}$ *x Cd4cre* mice 10 d after KLH immunization. (C) PNA staining of mLNs from WT and *Nfat2*$^{fl/fl}$ *x Cd4cre* mice 10 d after KLH immunization (top). Bars, 250 µm. Quantification of PNA-positive GC areas (bottom left) and percentage of PNA-positive follicles per mLN (bottom right) from 5 individual mice; PBS ctrl., mice received only PBS. (D) Representative flow cytometry of splenic and mLN GC-B cells from WT littermate and *Nfat2*$^{fl/fl}$ *x Cd4cre* mice 10 d after KLH immunization (left), plus synopsis of 12 independent experiments (right). (E) ELISA of NP-specific IgM, IgG1, and IgG3 antibodies in sera of WT and *Nfat2*$^{fl/fl}$ *x Cd4cre* mice before (non-immune) and after 10 d of NP-KLH immunization; each dot represents one individual mouse. (A and C–E) Student's *t* test: *, $P < 0.05$; **, $P < 0.005$.

CXCR5 expression is selectively impaired in NFAT2-deficient Foxp3$^+$ T_{reg} cells

As Foxp3 expression is independent on NFAT factors in thymus-derived nT_{reg} cells (Vaeth et al., 2012), we reasoned that NFAT2-deficient nT_{reg} cells might be unable to home to GCs. Indeed, when evaluating the frequency of Foxp3$^+$ cells in naive $CD4^+ICOS^-CXCR5^-$ or activated $CD4^+ICOS^{hi}CXCR5^-T_{conv}$ and $CD4^+ICOS^{hi}CXCR5^{hi}$ T_{FH} subsets from WT and *Nfat2*$^{fl/fl}$ *x Cd4cre* mice, the decrease in T_{FR} cells was paralleled by an increase in nT_{reg} cells within the $CD4^+ICOS^{hi}CXCR5^-$ (T_{act}) population (Fig. 6 A). This was a particular feature of NFAT2 and not affected by NFAT1 deficiency in Foxp3$^+$ T_{reg} cells of an activated $CD4^+CD44^{hi}$ phenotype (Fig. 6 B). Because CXCR5 is the essential homing receptor for T_{FH} and T_{FR} cells,

Published March 3, 2014

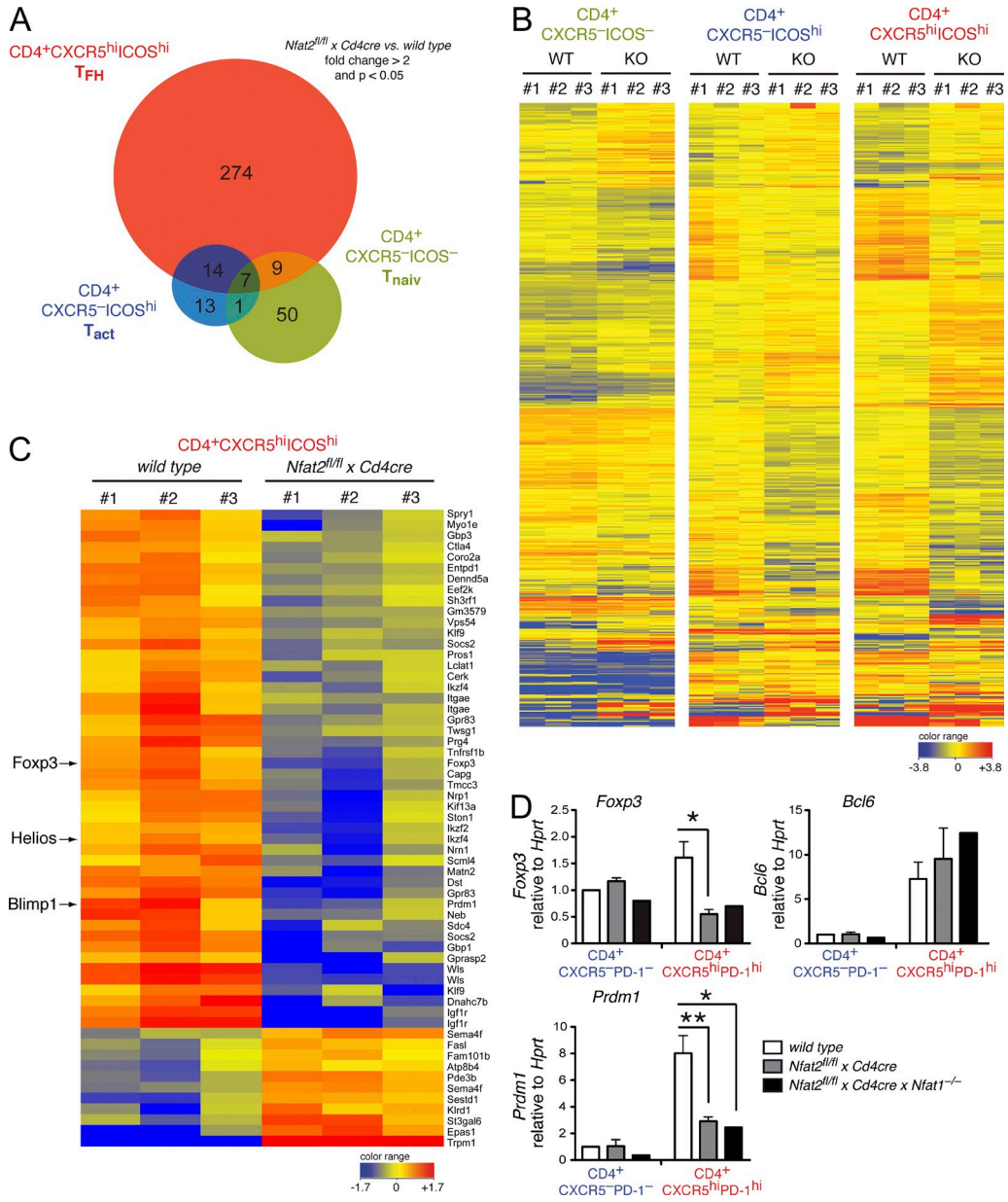

Figure 3. Global transcription analysis of NFAT2-deficient T cell subsets reveals reduced Foxp3⁺ T_{reg} frequencies within follicular T cells. (A) Venn diagram illustrating the overlap of differentially expressed genes in CXCR5⁻ICOS⁻ (T_{naiv}), CXCR5⁻ICOS^{hi} (T_{act}), and CXCR5^{hi}ICOS^{hi} (T_{FH}) CD4⁺ T cells from WT and *Nfat2$^{fl/fl}$ x Cd4cre* mice after immunization with KLH for 7 d. Differentially expressed genes (≥2-fold regulated; $P < 0.05$) were identified by comparing WT cells to their *Nfat2$^{fl/fl}$* x *Cd4cre* counterparts. (B) Clustering analysis and heatmap of gene expression in T cell subsets as in A. The heat map illustrates the log2 transformed expression intensity of genes that are at least twofold regulated between the populations and a p-value ≤ 0.05 for the effect of genotype. (C) Heatmap of T_{reg}-specific or -associated genes that are differentially expressed (≥2-fold; $P < 0.05$) between WT and NFAT2-deficient CD4⁺CXCR5^{hi}ICOS^{hi} T_{FH} cells. (A–C) Data are derived from 3 independent experiments with 12 mice per group and experiment. (D) qRT-PCR analysis of *Foxp3*, *Prdm1*, and *Bcl6* expression in FACS-sorted CXCR5⁺PD-1⁻ (T_{conv}) and CXCR5^{hi}PD-1^{hi} (T_{FH}) CD4⁺ T cells from KLH-immunized WT, *Nfat2$^{fl/fl}$ x Cd4cre*, and *Nfat2$^{fl/fl}$* x *Cd4cre* x *Nfat1$^{-/-}$* mice; 2 independent experiments each with 4 mice per group (two-way ANOVA: *, $P < 0.05$; **, $P < 0.005$).

we evaluated whether its expression differs in WT and NFAT2-deficient T cells. Therefore, we defined follicular T cells as CD4⁺BTLA^{hi} and found that NFAT2 selectively regulates CXCR5 expression in T_{FR} but not in T_{FH} cells (Fig. 6 C). In line with a T_{FR} cell–specific effect, transwell experiments suggested an impairment (although highly variable and therefore not significant) of NFAT2-deficient Foxp3⁺ nT_{reg} cells, but not T_{conv} cells from immunized littermate mice in migration toward a CXCL13 gradient (Fig. 6 D). Altogether, these data indicate that Foxp3⁺ nT_{reg} cells specifically depend on NFAT2 expression for the up-regulation of CXCR5.

Published March 3, 2014

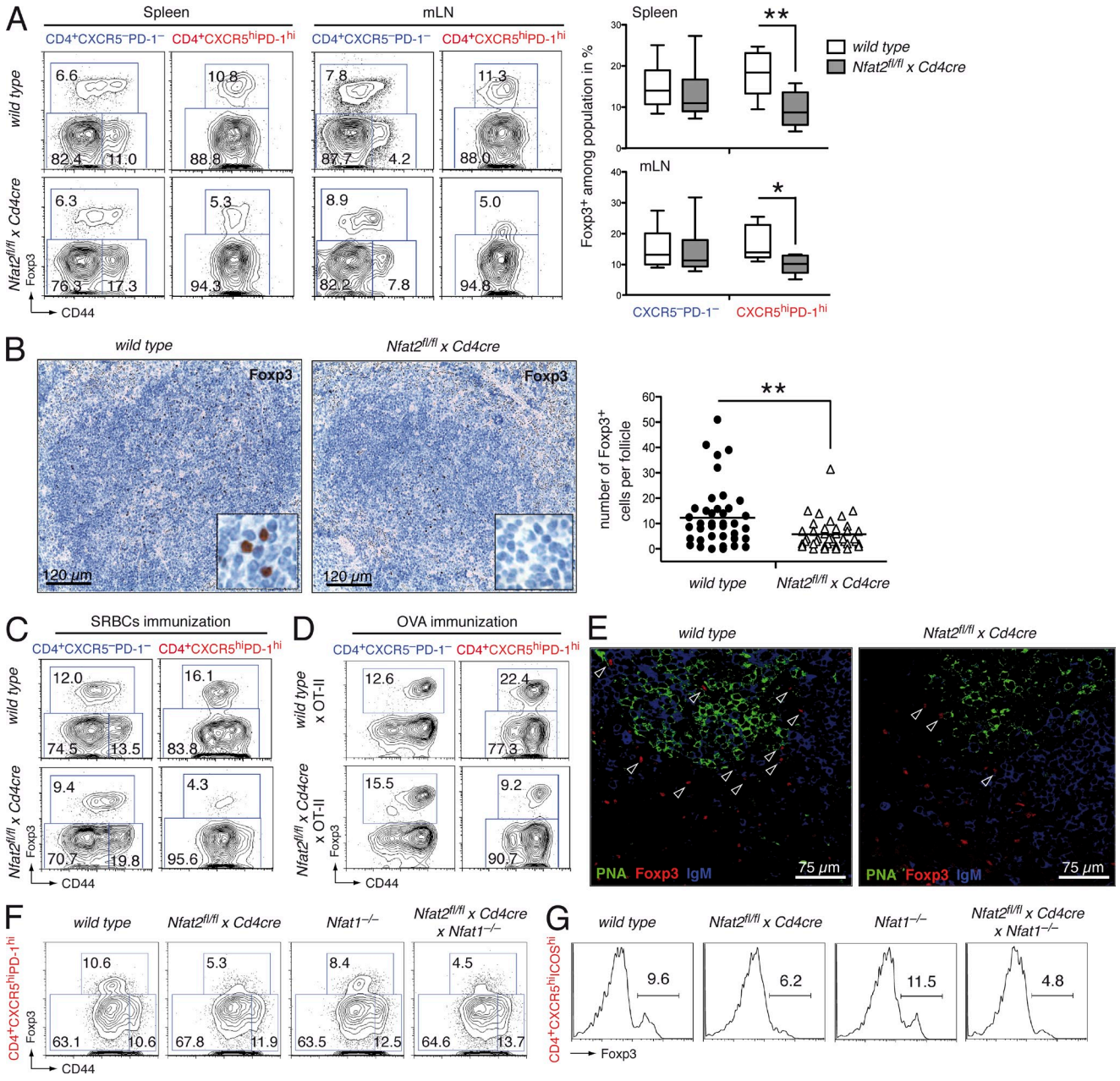

Figure 4. Impaired homing to B cell follicles of NFAT2-deficient Foxp3⁺ regulatory T cells augments GC reaction. (A) Flow cytometry of Foxp3⁺ T_{reg} frequency among CXCR5⁻PD-1⁻ (T_{conv}) and CXCR5^{hi}PD-1^{hi} (T_{FH}) CD4⁺ T cell populations in spleen and mLNs from KLH-immunized WT and *Nfat2$^{fl/fl}$ x Cd4cre* mice (left), plus summary of eight individual experiments (right). (B) Histological examination of Foxp3⁺ T_{reg} numbers in B cell follicles of KLH-immunized WT and *Nfat2$^{fl/fl}$ x Cd4cre* mice (left). Bars, 120 µm. Quantification of Foxp3⁺ cell numbers in follicles of four independent WT littermate and *Nfat2$^{fl/fl}$ x Cd4cre* littermates after KLH immunization (right); at least 10 follicles per individual spleen were analyzed. (A and B) Student's *t* test *, $P < 0.05$; **, $P < 0.005$. (C) Representative flow cytometry of Foxp3⁺ T_{reg} cells among CXCR5⁻PD-1⁻ (T_{conv}) and CXCR5^{hi}PD-1^{hi} (T_{FH}) splenic CD4⁺ T cell populations from SRBCs immunized WT and *Nfat2$^{fl/fl}$ x Cd4cre* mice. (D) Flow cytometry of Foxp3⁺ T_{reg} cells among CXCR5⁻PD-1⁻ (T_{conv}) and CXCR5^{hi}PD-1^{hi} (T_{FH}) splenic CD4⁺ T cell populations from OVA-immunized OT-II and *Nfat2$^{fl/fl}$ x Cd4cre x* OT-II mice. (E) Confocal microscopy of Foxp3 (red), IgM (blue), and PNA-positive cells (green) in splenic GCs of KLH-immunized WT and *Nfat2$^{fl/fl}$ x Cd4cre* mice. Bars, 75 µm. (F) Flow cytometry of Foxp3⁺ T_{reg} cell frequency among CD4⁺CXCR5^{hi}PD-1^{hi} T_{FH} cell population in spleens of KLH-immunized WT, *Nfat2$^{fl/fl}$ x Cd4cre*, *Nfat1$^{-/-}$*, and *Nfat2$^{fl/fl}$ x Cd4cre x Nfat1$^{-/-}$* mice. (G) Flow cytometry of Foxp3⁺ T_{reg} cells among CD4⁺ICOS^{hi}CXCR5^{hi} T_{FH} cells in spleens of KLH-immunized WT, *Nfat2$^{fl/fl}$ x Cd4cre*, *Nfat1$^{-/-}$*, and *Nfat2$^{fl/fl}$ x Cd4cre x Nfat1$^{-/-}$* mice.

CXCR5-competent nT_{reg} cells rescue the NFAT2-deficient phenotype

Although CXCR5 expression was clearly dependent on the presence of NFAT2, this could have been just one among many decisive reasons for a dysregulated GC reaction. In line with the notion that the observed defect laid within the nT_{reg} compartment, adoptive transfer of in vitro anti-CD3/CD28-activated congenic WT nT_{reg} cells into immunized WT or

Published March 3, 2014

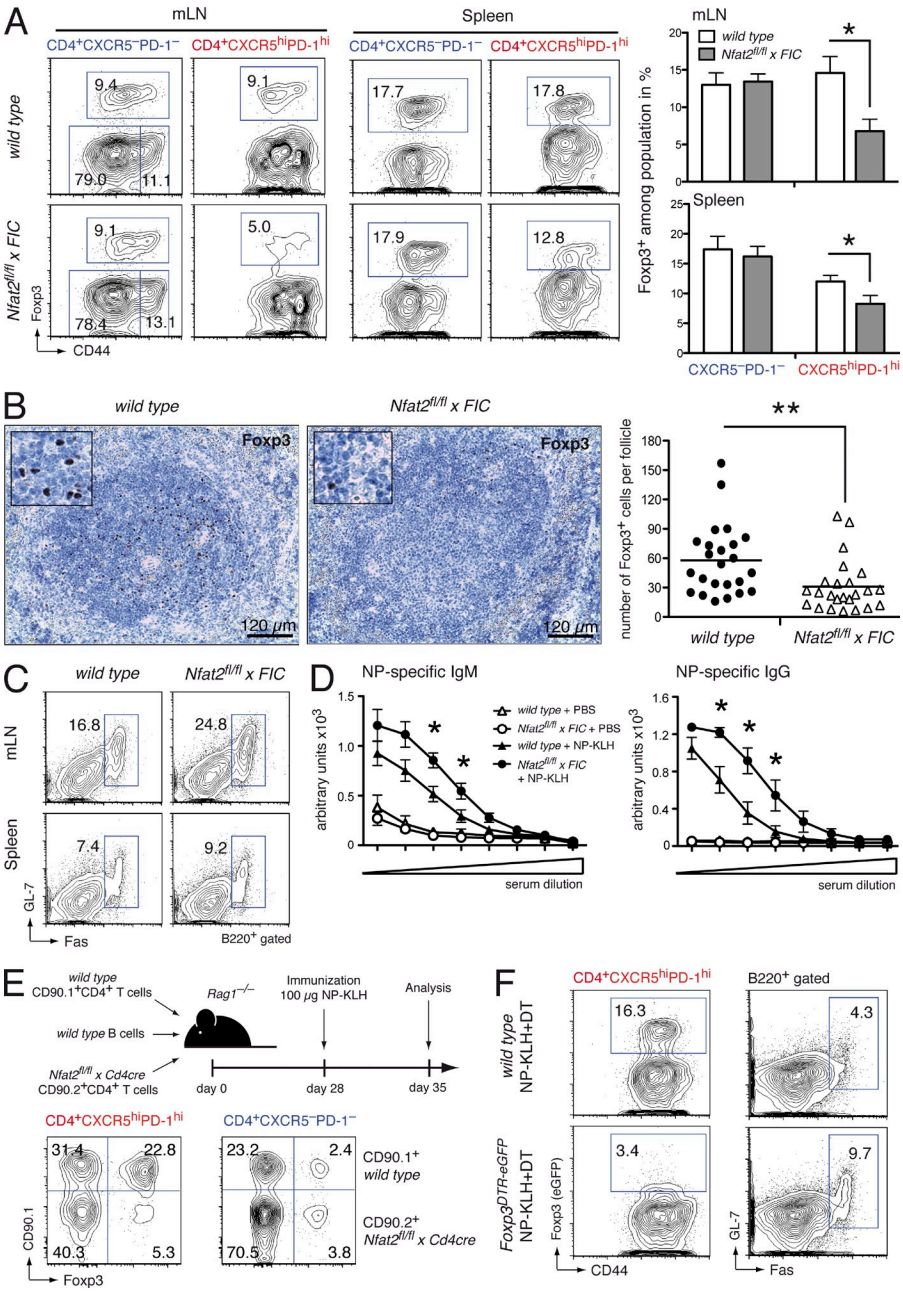

Figure 5. Impaired homing of Foxp3+ regulatory T cells to B cell follicles is a T_{reg} cell–intrinsic, NFAT2-regulated defect. (A) Flow cytometry of Foxp3+ T_{reg} cell frequency among CXCR5-PD-1- (T_{conv}) and CXCR5hiPD-1hi (T_{FH}) CD4+ T cell populations in spleen and mLN from KLH-immunized WT and *Nfat2fl/fl x Foxp3-IRES-Cre* (*FIC*) mice (left), plus summary of five independent experiments (right). (B) Histological examination of Foxp3+ T_{reg} numbers in B cell follicles of KLH-immunized WT littermate and *Nfat2fl/fl x FIC* mice (left). Bars, 120 µm. Quantification of Foxp3+ cell numbers per follicle from three independent WT and *Nfat2fl/fl x FIC* littermates after KLH immunization (right). (C) Representative flow cytometry of splenic and mLN GC-B cells from WT and *Nfat2fl/fl x FIC* mice 10 d after KLH immunization. (D) ELISA of NP-specific IgM and IgG antibodies in sera (three-fold dilution steps starting from a 1:20 initial dilution) of WT and *Nfat2fl/fl x FIC* littermates after 10 d of NP-KLH immunization or PBS as control; 3 individual mice per group; $n = 5$ for both ELISA. (E) Scheme of adoptive co-transfer of 12 × 10^6 WT B cells, 6 × 10^6 CD90.1+ CD4+ WT T cells, and 6 × 10^6 CD90.1+CD4+ *Nfat2fl/fl x Cd4cre* T cells into *Rag1−/−* mice followed by KLH immunization (top). Representative FACS analysis of Foxp3+ T_{reg} cells within CD90.1+ or CD90.2+ population among CXCR5-PD-1- (T_{conv}) and CXCR5hi PD-1hi (T_{FH}) CD4+ T cells in mLNs from *Rag1−/−* hosts (bottom). (F) KLH immunization of WT and *Foxp3DTR-eGFP* (DEREG) mice followed by depletion of (follicular) T_{reg} cells using diphtheria toxin (DT). Flow cytometry of CXCR5hiPD-1hi follicular T cells and GC-B cells. (A, B, and D) Student's *t* test: *, $P < 0.05$; **, $P < 0.005$.

Nfat2fl/fl x Cd4cre recipient mice complemented the reduced number of T_{FR} cells in NFAT2-deficient mice and rescued the GC phenotype (Fig. 7 A). Therefore, *Nfat2−/−* nT_{reg} cells were lentivirally transduced for CXCR5-GFP expression and adoptively transferred together with B cells and naive T_{conv} cells into *Rag1−/−* mice, which were immunized 2 wk thereafter (Fig. 7 B). Pre-activated NFAT2-deficient (in parallel with NFAT2-sufficient) nT_{reg} cells were successfully manipulated to express CXCR5 at their surface (Fig. 7 C). In fact, this made up for their NFAT2 deficiency during the provoked GC-reactions and restored GC-B cell numbers to normal levels (Fig. 7 D).

NFAT2 transactivates *Cxcr5*

Computational analyses of the TATA-less *Cxcr5* promoter region revealed three conserved noncoding sequences (CNS) between men, dog, and mice with putative NFAT responsive elements (Fig. S1, A and B). Furthermore, two DNase hypersensitive sites (HS1 and HS2) could serve as 3′ enhancers (Fig. S1 C). Reporter gene assays in human Jurkat T or murine EL-4 thymoma cells using a −1,127-bp fragment of the *Cxcr5* promoter region containing most putative NFAT-responsive elements demonstrated inducibility and sensitivity to CsA (Fig. 8, A and B). Here, cells were activated by TPA plus ionomycin (T/I), which mimics antigen-receptor engagement.

Published March 3, 2014

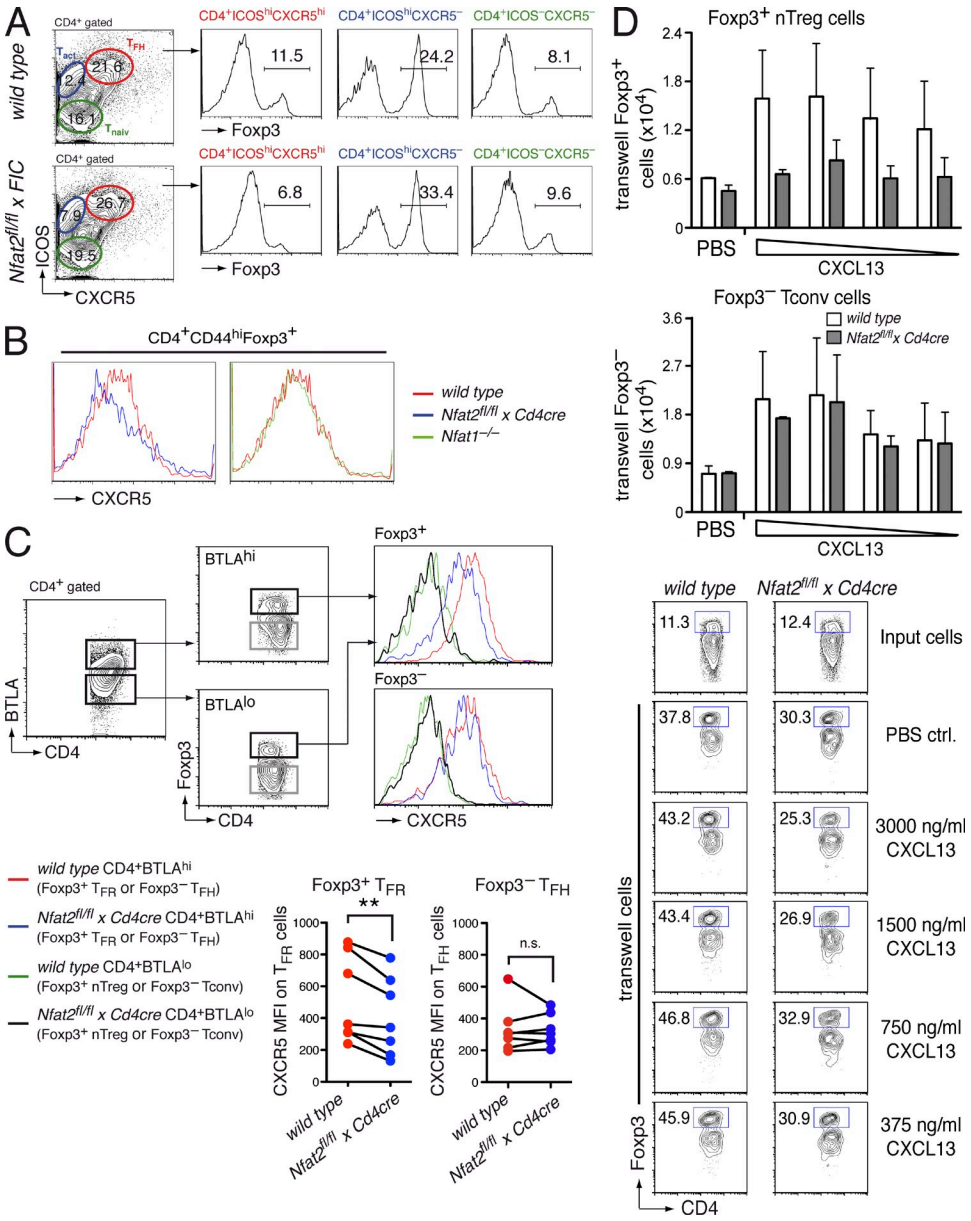

Figure 6. *Cxcr5* expression depends on NFAT2 only in T_{FR} cells. (A) Flow cytometry of Foxp3$^+$ T_{reg} cells among CXCR5$^-$ICOS$^-$ (T_{naiv}), CXCR5$^-$ICOS^{hi} (T_{act}), and CXCR5^{hi}ICOS^{hi} (T_{FH}) mLN CD4$^+$ T cells from KLH-immunized WT and *Nfat2$^{fl/fl}$ x FIC* mice. (B) Surface expression of CXCR5 on splenic CD4$^+$CD44^{hi}Foxp3$^+$ T_{reg} cells from KLH-immunized WT, *Nfat2$^{fl/fl}$ x Cd4cre*, and *Nfat1$^{-/-}$* mice. (C) Expression of CXCR5 on BTLA^{hi}Foxp3$^+$, BTLA^{lo}Foxp3$^+$, BTLA^{hi}Foxp3$^-$, and BTLA^{lo}Foxp3$^-$ splenic CD4$^+$ T cells of KLH-immunized WT and *Nfat2$^{fl/fl}$ x Cd4cre* littermates using flow cytometry; MFI of CXCR5 expression is quantified below (Student's *t* test; **, $P < 0.005$). (D) Transwell assay of CD4$^+$ T cells and CD4$^+$Foxp3$^+$ T_{reg} cells in vitro (two independent experiments; two-way ANOVA, ns). Total number of CD4$^+$Foxp3$^+$ T_{reg} cells and CD4$^+$Foxp3$^-$ T_{conv} cells from KLH-immunized WT littermate and *Nfat2$^{fl/fl}$ x Cd4cre* mice in the bottom transwell after 5-h incubation with various concentrations of CXCL13 (left). Phenotype of input and transwell cells after 5-h incubation with various concentrations of CXCL13 analyzed by flow cytometry (right).

The presence of HS2 slightly enhanced, but did not influence the quality of activity (Fig. 8 A). Within the *Cxcr5* promoter three conserved regions (named as proximal, middle, and distal regions; Fig. S1, A and B) were defined, each containing putative NFAT-responsive elements (Fig. S1, B and D). To address if NFAT can bind to these sites, we performed electrophoretic mobility shift assays (EMSAs) using *Cxcr5-N1* to *Cxcr5-N4* as probes. Total protein extracts were prepared from transfections with an expression plasmid for the DNA-binding domain of NFAT2 (HA-Nc1-RSD; Klein-Hessling et al., 2008)). The most proximal site (*Cxcr5-N1*) showed a similar bandshift as the *Pubd* from the *Il2* promoter, but could not respond to Blimp-1, which recognizes a similar core consensus sequence, namely GAAAG (Kuo and Calame, 2004). *Cxcr5-N1*

Published March 3, 2014

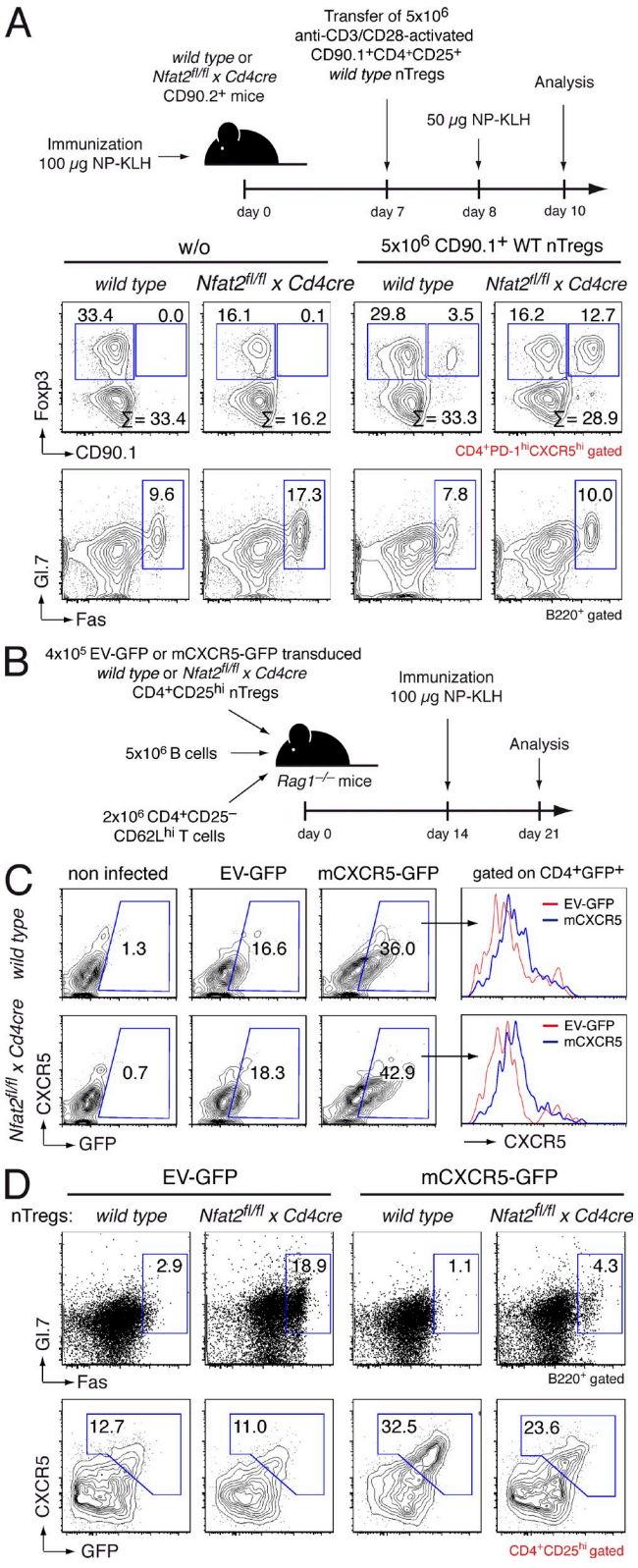

Figure 7. CXCR5-competent nT_{reg} cells rescue the NFAT2-deficient phenotype. (A) Activated WT nT_{reg} cells rescue the GC phenotype in NFAT2-deficient mice. Experimental layout transferring 5 × 10^6 anti-CD3/CD28 activated CD90.1+ congenic WT nT_{reg} cells in KLH-immunized CD90.2+ WT and *Nfat2*$^{fl/fl}$ *x Cd4cre* recipient mice (top). Analysis of host and donor T_{FR} cells and GC-B cells in mice with or without adoptive transfer of 5 × 10^6 CD90.1+ nT_{reg} cells using flow cytometry (bottom). (B–D) Lentiviral CXCR5 transduction of NFAT2-deficient nT_{reg} cells rescues the GC phenotype. (B) Scheme of adoptive transfer experiments using CXCR5-transduced WT and *Nfat2*$^{fl/fl}$ *x Cd4cre* nT_{reg} cells. (C) Anti-CD3/CD28-activated WT and NFAT2-deficient CD4+CD25hi nT_{reg} cells were transduced with lentiviruses encoding for murine CXCR5-GFP or GFP only (EV, empty vector); 4 d later transduction efficiency was analyzed by flow cytometry. (D) Analysis of GC reaction in *Rag1*$^{-/-}$ mice transferred with WT B cells and CD4+CD25-CD62Lhi T cells together with either mCXCR5-GFP– or EV-GFP–transduced WT and *Nfat2*$^{fl/fl}$ *x Cd4cre* nT_{reg} cells. FACS-analysis 21 d after transfer and 7 d after KLH immunization.

therefore assigns for a potent and specific NFAT-responsive element (Fig. 8 C). Using nuclear extracts from stimulated primary T_{reg} cells corroborated the strong binding of NFAT to *Cxcr5-N1*. Both NFAT1 and NFAT2 could be recruited to this site as demonstrated by anti-NFAT1– and anti-NFAT2–mediated supershifts (Fig. 8 D). Chromatin immunoprecipitation (ChIP) assays using T cells from WT and *Nfat2*$^{fl/fl}$ *x Cd4cre* mice immunized with KLH verified the proximal part of the *Cxcr5* promoter to be bound by NFAT2 in vivo (Fig. 8 E). To test the function of the *Cxcr5-N1* site, we deleted distal parts of the *Cxcr5* promoter and found that the proximal part alone (−329 bp, containing *Cxcr5-N1*) could mediate T/I induction in Jurkat cells (Fig. 8 F). Next, we mutated the two G-nucleotides of the *Cxcr5-N1* motif essential for NFAT-binding within the 1,127-bp-long promoter fragment (NFAT-mutated). When nonlymphoid human embryonic kidney (HEK 293T) cells were transfected, we found that exogenous NFAT2 transactivated the *Cxcr5* promoter robustly, but only when *Cxcr5-N1* was intact (Fig. 8 G and Fig. S1 D). In line with this, a significantly reduced induction was witnessed in Jurkat cells, when this single NFAT-responsive element was mutated (Fig. 8 H). The same tendency was observed for the 329-bp fragment, as shown for EL-4 cells (Fig. 8 I). Overall, this demonstrated the important role of *Cxcr5-N1* for NFAT2-mediated transactivation of *Cxcr5*.

NFAT2-deficient T_{FR} cells fail to control a lupuslike disease in chromatin-immunized mice

Patients suffering from SLE commonly exhibit increased frequencies of T_{FH} and GC-B cells and high titers of pathogenic auto-Abs (Simpson et al., 2010), often correlated with impaired numbers and function of T_{reg} cells (Valencia et al., 2007; Bonelli et al., 2008, 2010). Clinical hallmarks of SLE are antinuclear antigen (ANA) and anti–double-stranded DNA (dsDNA) auto-Abs. Accordingly, immunization with chromatin isolated from syngeneic-activated lymphocytes leads to a lupuslike disease in mice (Li et al., 2004; Qiao et al., 2005), which we performed with WT and *Nfat2*$^{fl/fl}$ *x Cd4cre* littermate mice (Fig. 9 A). Equivalent with all other immunizations, we observed a modestly increased number in CD4+CXCR5hiPD-1hi T_{FH} cells (unpublished data), as well as GL-7hiFAShi GC-B cells and, importantly, a sharp drop in

Published March 3, 2014

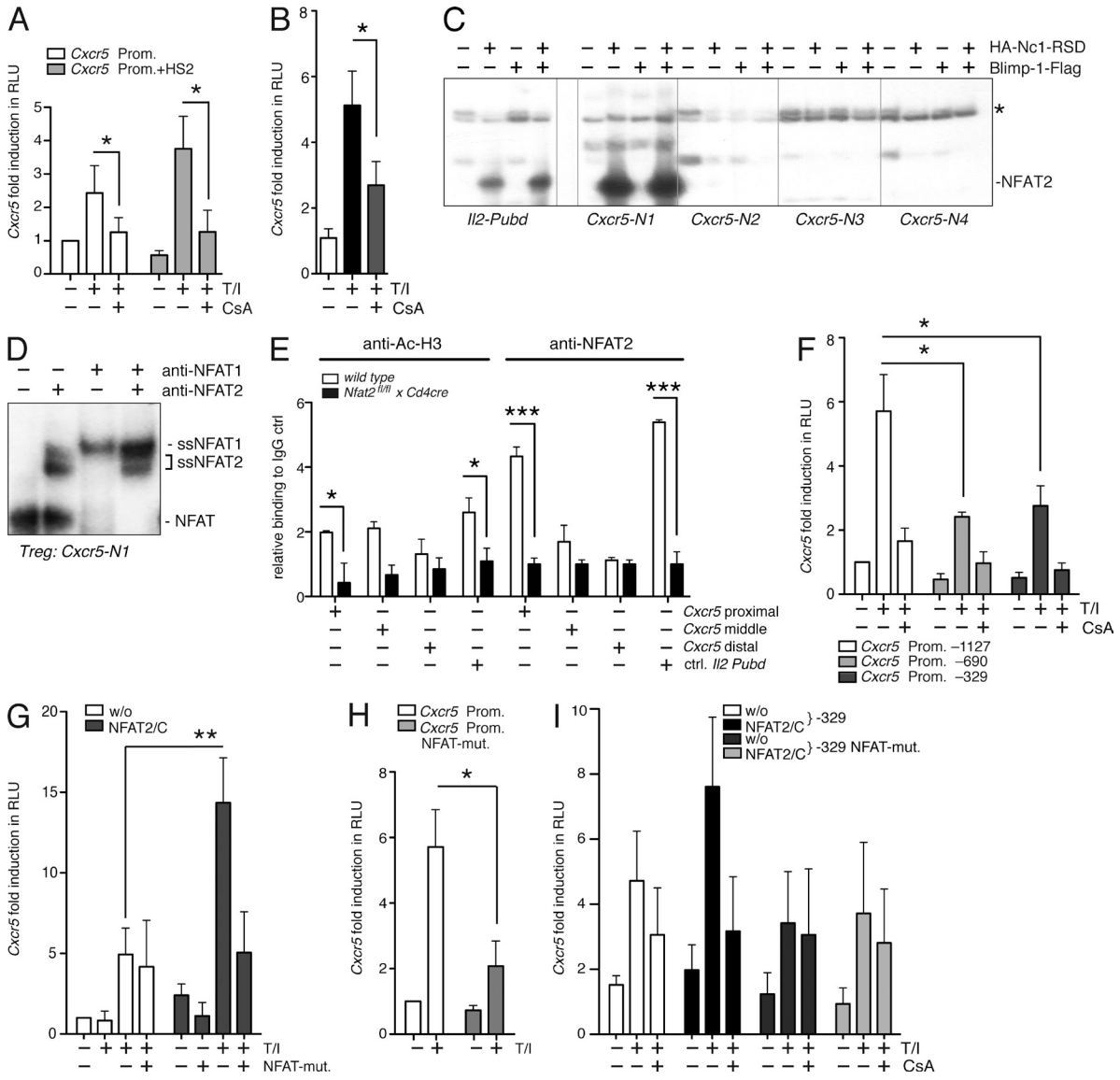

Figure 8. NFAT2 regulates *Cxcr5* expression in T cells. (A) Luciferase assays of the *Cxcr5* promoter and *Cxcr5* promoter plus HS2. Transiently transfected Jurkat cells were stimulated with T/I or T/I plus CsA; four independent experiments. Student's *t* test: *, $P < 0.05$. (B) Luciferase assay as in A, but with EL-4 cells and the *Cxcr5* promoter only; three independent experiments; Student's *t* test: *, $P < 0.05$. (C) EMSA with whole cell extracts from 293T HEK cells transiently transfected with Ha-Nc1-RSD (35 kD) or Blimp-1-Flag (98 kD) and *Il2-Pubd*, *Cxcr5-N1*, *Cxcr5-N2*, *Cxcr5-N3*, or *Cxcr5-N4* as probes (NFAT2, specific binding; *, unidentified band). (D) EMSAs with nuclear protein extracts from murine T_{reg} cells harvested after 48 h of anti-CD3/CD28 plus IL-2 stimulation using the *Cxcr5-N1* site as probe (position of NFAT-bound probe and antibody-supershifts [ss] are indicated). (E) ChIP analysis of NFAT2 binding to the proximal, middle, and distal parts of the *Cxcr5* promoter and the *Il2* promoter containing *Pubd*. WT and *Nfat2$^{fl/fl}$ x Cd4cre* mice were immunized with KLH for 7 d and splenic CD4$^+$ T cells were used; two-way ANOVA: *, $P < 0.05$; **, $P < 0.005$; ***, $P < 0.001$. (F) Luciferase assays of full-length *Cxcr5* promoter (−1,127) and truncated versions (−690 and −329). Transiently transfected Jurkat cells were stimulated with T/I or T/I plus CsA; 4 independent experiments; Student's *t* test: *, $P < 0.05$. (G) Luciferase assays of full-length *Cxcr5* promoter (−1,127) of WT or mutated proximal *Cxcr5-N1* NFAT motif (NFAT-mutated). HEK 293T cells were transiently co-transfected with empty vector or a NFAT2/C construct; 6 independent experiments; two-way ANOVA: *, $P < 0.05$; **, $P < 0.005$. (H) Luciferase assays of full-length *Cxcr5* promoter (−1,127) of WT or mutated proximal *Cxcr5-N1* NFAT motif (NFAT-mutated). Transiently transfected Jurkat cells were stimulated with T/I; 4 independent experiments; Student's *t* test: *, $P < 0.05$. (I) Luciferase assays of the proximal *Cxcr5* promoter (−329) of WT or mutated proximal *Cxcr5-N1* NFAT motif (NFAT-mutated). EL-4 cells were transiently transfected with empty vector or an NFAT2/C construct and stimulated with T/I or T/I plus CsA; 3 independent experiments; two-way ANOVA, n.s.

the frequency of T_{FR} cells in spleen and mLN (Fig. 9 B and not depicted). Consequently, titers of pathogenic anti-dsDNA auto-Abs were found to be increased upon T cell–specific loss of NFAT2 (Fig. 9 C). PNA-immunohistochemistry of chromatin-immunized mice exhibited enlarged splenic B cell follicles in *Nfat2$^{fl/fl}$ x Cd4cre* mice (unpublished data). Indicative of a lupuslike disease, PAS-staining detected increased intracapillary, mesangial hypercellularity and thickened contours of

Published March 3, 2014

the mesangial matrix in kidney sections of NFAT2-deficient mice (Fig. 9 D). Furthermore, detection of pathogenic immunoglobulin deposition in the kidneys was indicative of an aggravated lupuslike disease in chromatin-immunized *Nfat2*$^{fl/fl}$ *x Cd4cre* mice (Fig. 9 E). All these data demonstrate that NFAT2 is essential for T_{FR} cells to control humoral autoimmunity.

DISCUSSION

Earlier transcriptional profiling of CD4$^+$ICOS^{hi}CXCR5^{hi} T_{FH} cells from chronically inflamed tonsils identified *Nfat2* as one of the most prominently up-regulated genes (Rasheed et al., 2006). When we now analyzed murine T_{FH} cells we found a similar prevalence of NFAT2 among transcription factors in general and NFAT members especially. Immunization of mice, in which *Nfat2* was specifically ablated in T cells, resulted in an unexpected phenotype, i.e., an enhanced GC reaction. This could be tracked down to an impairment of Foxp3$^+$ T_{reg} cells to up-regulate CXCR5, leading to reduced numbers of Foxp3$^+$ T_{FR} cells within GCs. NFAT2-dependent CXCR5 up-regulation and consequential homing to GCs was T_{FR} cell–intrinsic as well as specific. Furthermore, rescue experiments verified that the inability to induce CXCR5 in nT_{reg} cells accounted for the observed phenotype. Therefore, absence of NFAT2 was sufficient to exclude T_{FR} cells from GCs. The outstanding importance for precise homing of CXCR5^{hi}Foxp3$^+$ T_{FR} cells was emphasized in a murine model of a lupuslike disease with a boosted severity in the absence of NFAT2.

One possible interpretation of the enhanced GC reaction upon *Nfat2* ablation in T cells might have taken into account that NFAT proteins are decisive transactivators of *Il2* and that less IL-2 favors GC formation (Ballesteros-Tato et al., 2012; Johnston et al., 2012). However, (a) single deficiency of NFAT2 does not dramatically reduce the levels of IL-2 (Vaeth et al., 2012), (b) we confirmed the increase of T_{FH} and GC-B cells after T_{reg}-specific deletion of *Nfat2*, (c) demonstrated the reduction of CXCR5 on T_{reg} cells as cell-intrinsic by co-transferred WT and *Nfat2*$^{-/-}$ CD4$^+$ T cells, and (d) were able to rescue the overshooting GC reaction in *Nfat2*$^{fl/fl}$ *x Cd4cre* mice by transfer of CXCR5-sufficient WT nT_{reg}cells.

Still, the phenotype of T cell–specific *Nfat2* ablation, which is dominated by *Nfat2*$^{-/-}$ T_{reg} cells, was unexpected, as we had revealed that overall frequency and distribution of nT_{reg} cells remains unaltered in mice that were NFAT2-deficient upon thymic CD4 expression (Vaeth et al., 2012). However, the observed augmented GC formation correlated with an exclusive decrease in T_{FR} cells and could be reversed by an adoptive transfer of WT and NFAT2-deficient, but CXCR5-sufficient, nT_{reg} cells. Consistently, nT_{reg} cells were selectively affected in up-regulating the chemokine receptor CXCR5. CXCR5 empowers T cells to migrate toward a CXCL13 gradient and accumulate site-specifically within GCs. This is reminiscent of expression of the Th1-defining transcription factor T-bet in nT_{reg} cells, leading to CXCR3 induction and migration to sites of Th1 responses, or of STAT3 induction for adapting CCR6 expression like Th17 cells (Chaudhry et al., 2009; Josefowicz et al., 2012; Koch et al., 2009). Therefore, the specific high expression of NFAT2 in GC-B, T_{FH}, and, concomitantly, in T_{FR} cells is another example of transcription factor cooption allowing T_{reg} cells to suppress distinct immune responses (Josefowicz et al., 2012).

So far, Bcl-6, which is obligatory for GC-B and T_{FH} cells, had been designated as the coopting transcription factor in T_{FR} cells, as it is mainly responsible for CXCR5 expression (Chung et al., 2011; Linterman et al., 2011; Josefowicz et al., 2012). However, ectopic expression of Bcl-6 is insufficient to drive CXCR5 expression (Ma et al., 2012). Strikingly, transferred naive CD4$^+$ T cells from *Bcl6*$^{-/-}$ mice exhibit the same CXCR5 induction as WT cells, although T_{FH} cells depend on Bcl-6 for a stable lineage commitment (Liu et al., 2012). Because Bcl-6 acts as a repressor, it instead intervenes with the transcriptional fate of other CD4$^+$ T cell lineages; e.g., it antagonizes GATA3 expression and Th2 responses (Kusam et al., 2003) and *Tbx21* and *Rorc* expression (Yu et al., 2009), or binds and inhibits T-bet protein (Oestreich et al., 2012). Therefore, follicular T cell specificity is provided indirectly by Bcl-6.

Currently, little is known about the transcriptional control of *Cxcr5* in T_{FH} and T_{FR} cells. In mature B cells, constitutive expression is cooperatively regulated by Oct-2, Bob1 (OBF-1), and NF-κB, which bind to consensus sequences within its proximal promoter (Wolf et al., 1998). In addition, a putative NFAT-responsive element (*Pu.box*) was recognized. Indeed, in retinoic acid–treated HL-60 cells, the human homologous element binds NFAT4 (Wang and Yen, 2004). However, we could not detect any binding of NFAT proteins to the murine *Cxcr5-N3*. Another putative site, *Cxcr5-N2*, is essential for NF-κB responsiveness in B cells (Wolf et al., 1998), in line with a high degree of overlap between NFAT and NF-κB sites (McCaffrey et al., 1994). Importantly, the most proximal and thus far unrecognized *Cxcr5-N1* proofed to be a true and decisive NFAT response element. Therefore, NFAT2 is likely to contribute to CXCR5 expression in GC-B and T_{FH} cells.

The fact that only T_{FR}, but not T_{FH} cells depend on NFAT2 to migrate to GCs attributes to the special transcriptional landscape of nT_{reg} cells. Effector T_{reg} (eT_{reg}) cells, which have differentiated in parallel with their respective T_{conv} cells highly express Blimp-1 in addition to Foxp3 (Cretney et al., 2013). From PCs it is known that Blimp-1 represses CXCR5, which is a requisite to egress from GCs (Shaffer et al., 2002). Similarly, Blimp-1 deletion (Linterman et al., 2011) led to an up-regulation of CXCR5, whereas overexpression of Blimp-1 repressed CXCR5 (Oestreich et al., 2012). One possibility also supported by our preliminary data could be that NFAT2 specifically overcomes the Blimp-1–mediated repression in T_{FR} cells. In such a scenario, this molecular checkpoint would be controlled by an inhibiting (i.e., Blimp-1) and activating (i.e., NFAT2) factor, which ensures an adequate expression of CXCR5, and thereby an appropriate GC response. A mutual balancing of Blimp-1 and NFAT2 might even culminate in synergy. At least this has been described for eT_{reg} cells, where Blimp-1 in conjunction with IRF4 acts as a positive regulator at the *Il10* intron1 enhancer (Cretney et al., 2011).

Published March 3, 2014

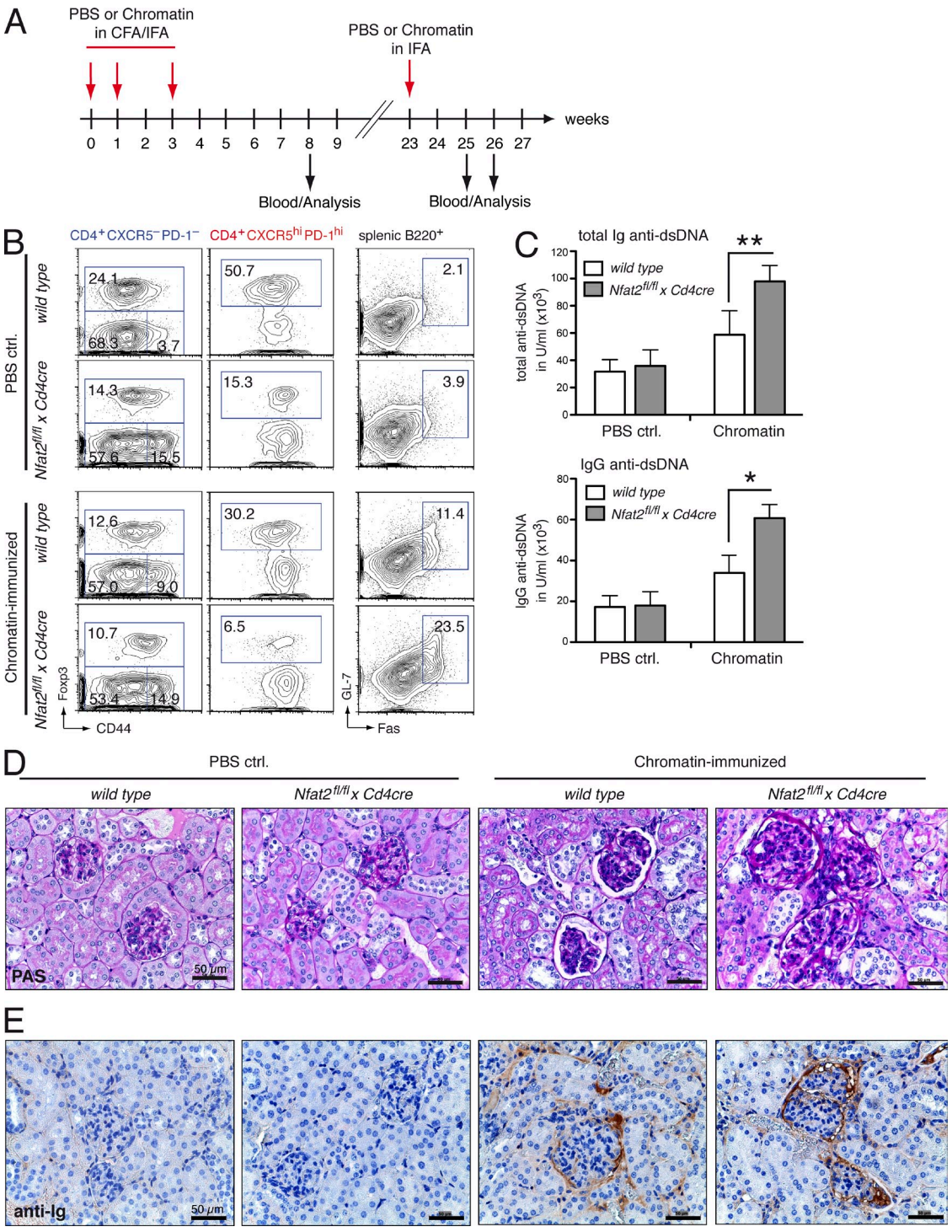

Figure 9. NFAT2-deficient Foxp3⁺ regulatory T cells fail to control a lupuslike disease in chromatin-immunized mice. (A) Schedule of PBS and chromatin immunization to provoke a lupuslike disease in WT littermate and *Nfat2$^{fl/fl}$ x Cd4cre* mice. (B) Flow cytometry of CXCR5^{-}PD-1^{-} conventional, CXCR5^{hi}PD-1^{hi} follicular T cells, and GC-B cells in spleens of immunized mice. WT and *Nfat2$^{fl/fl}$ x Cd4cre* littermates were immunized with PBS in CFA (PBS ctrl.) or chromatin in CFA and analyzed 8 wk after first immunization. (C) ELISA for dsDNA-specific total immunoglobulins (top) and IgG (bottom) in sera of PBS or chromatin immunized WT littermate and *Nfat2$^{fl/fl}$ x Cd4cre* mice. Sera from 5 individual mice were analyzed 8 wk after first immunization. Student's *t* test: *, $P < 0.05$; **, $P < 0.005$. (D) PAS staining of kidney samples from PBS in CFA (PBS ctrl.) or chromatin in CFA-immunized WT and *Nfat2$^{fl/fl}$ x Cd4cre* mice 25 wk after immunization. Bars, 50 µm. (E) Histological analysis of immunoglobulin deposition in kidneys of WT and *Nfat2$^{fl/fl}$ x Cd4cre* littermates 25 wk after PBS or chromatin immunization. Bars, 50 µm.

Published March 3, 2014

T_{reg} cells can directly suppress B cells in GCs and periphery (Lim et al., 2005; Vaeth et al., 2011; Sage et al., 2013), where T_{reg}-derived IL-10 and the GITR are functionally involved (Alexander et al., 2011). In addition, we found that direct cell–cell contact enables the transfer of cAMP (cyclic adenosine monophosphate) from T_{reg} into B cells via gap-junction intracellular communication, resulting in the induction of ICER (inducible cAMP early repressor; Bopp et al., 2007; Vaeth et al., 2011; Bodor et al., 2012). ICER is a transcriptional repressor, which inhibits lymphocyte activation not only by interfering with *Nfat2* expression directly, but also the suppression of NFAT-mediated transcription (Vaeth et al., 2011; Bodor et al., 2012). Because GC-B cells require high levels of NFAT2 for GC formation and the production of class-switched, high-affinity Abs (Bhattacharyya et al., 2011), the inhibition of NFAT in target cells appears as an additional mechanism in how T_{FR} cells regulate GC reaction.

In summary, NFAT2 is instrumental for both an adequate and nonpathological humoral immune response. Whereas NFAT2 is of importance for GC-B and T_{FH} cells (Rasheed et al., 2006; Bhattacharyya et al., 2011), it is concomitantly needed to limit the GC reaction by T_{FR} cells. NFAT2 regulates the specific homing of T_{FR} cells to GCs via up-regulating CXCR5, essentially to prevent humoral autoimmune diseases like SLE.

MATERIALS AND METHODS

Mice and cells. *Nfat2*$^{fl/fl}$ mice were generated in A. Rao's laboratory (Harvard Medical School, Boston, MA). Phenotypes, when crossed to *Cd4cre* and *FIC,* have been explored earlier and proof of NFAT2 deficiency had previously been provided on genetic and protein levels for all T cells including nT_{reg} cells (Vaeth et al., 2012). *Nfat1*$^{-/-}$, *Nfat4*$^{-/-}$, B6-Tg (*Cd4cre*) 1Cwi/Cwilbcm (EMMA, Italy), *Foxp3-IRES-cre* (*FIC*), *OT-II*, *Rag1*$^{-/-}$, *Nfatc1/egfp*, and *Foxp3*$^{DTR\text{-}eGFP}$ (DEREG) mice have been described (Barnden et al., 1998; Ranger et al., 1998; Lee et al., 2001; Jasinski et al., 2006, Lahl et al., 2007; Wing et al., 2008; Hock et al., 2013). Animals were used at 6 to 16 wk and maintained in accordance with institutional guidelines for animal welfare. Jurkat, EL-4, and HEK 293T cells were cultured in complete RPMI or DMEM medium containing 10% FCS (Nayak et al., 2009; Vaeth et al., 2012).

Immunizations, T_{reg} depletion, and adoptive cell transfer. Sex-matched littermate mice were immunized (approval by the government of Lower Franconia; 55.2–2531.01-80/10) intraperitoneally (i.p.) with 100 µg NP-(27)-KLH (BioCat) emulsified in Imject Alum (Thermo Fisher Scientific) or 10^9 SRBCs (Dunn Labortechnik) and analyzed on d 7. In some experiments, mice were boosted with 50 µg NP-(27)-KLH on day 7 and analyzed on d 10–12. OT-II mice were immunized i.p. with 100 µg $OVA_{323\text{-}339}$ emulsified in Imject Alum. Depletion of Foxp3$^+$ T_{reg} cells in *Foxp3*$^{DTR\text{-}eGFP}$ (DEREG) mice was performed by daily injection of 1 µg diphtheria toxin (DT) in PBS i.p. on day 1–3 after KLH immunization. For adoptive cell transfer experiments, 12×10^6 negatively isolated WT B cells (Miltenyi Biotec) were transferred along with 6×10^6 WT negatively isolated (Invitrogen) CD90.1$^+$CD4$^+$ T cells and 6×10^6 CD90.1$^+$CD4$^+$ *Nfat2*$^{fl/fl}$ *x Cd4cre* T cells i.p. into *Rag1*$^{-/-}$ mice. After 28 d mice were immunized with 100 µg NP-(27)-KLH. For rescue experiments, CD90.1$^+$CD4$^+$CD25$^+$ WT nT_{reg} cells were isolated and activated with anti-CD3/CD28 beads (Invitrogen). 7 d after immunization, 5×10^6 nT_{reg} cells were injected retroorbitally into CD90.2$^+$ WT and *Nfat2*$^{fl/fl}$ *x Cd4cre* littermates.

Chromatin immunization. Induction of a lupuslike disease by chromatin immunization was performed as reported by others (Li et al., 2004; Qiao et al., 2005). In brief, chromatin was isolated from syngenic BL/6 splenocytes stimulated for 2 d in complete RPMI with T/I. After washing, nuclei were extracted, washed, and lysed in buffer containing 300 mM NaCl, 25 mM EDTA, 50 mM Tris-HCl, pH 8.0, 0.2% SDS, and 0.5 mg/ml Proteinase K (Fermentas) overnight at 50°C. Chromatin was precipitated with EtOH, dried, and digested by incubation with S1 Nuclease (Fermentas) for 60 min at 30°C in the respective buffer. The reaction was stopped by addition of 40 mM EDTA for 15 min at 70°C and the chromatin was finally precipitated with EtOH, dried, and resolved in PBS at 1 µg/µl concentration. Mice were immunized subcutaneously (s.c.) with 100 µg chromatin in 100 µl CFA (Difco) and the immune reaction was boosted with additional s.c. injection of 100 µg chromatin in IFA (Difco) in the 1st, 3rd, and 23rd week.

Antibodies for flow cytometry and FACS-sorting. FACS staining was performed with following Abs: FITC-conjugated CD4 (GK1.5), CD44 (IM7), CD90.1 (OX-7), CXCR4 (2B11), GL-7 (Ly-77); PE-conjugated CD4 (RM4-5), CD19 (1D3), CD25 (PC61), CD95/Fas (DX2), CD272/BTLA (8F4), CD279/PD-1 (RMP1-30), CXCR5 (2G8); biotin-conjugated B220 (RA3-6B2), CD4 (GK1.5) CD90.2 (53–2.1), CXCR5 (SPRCL5), ICOS (7E.17G9); eFluor 450-conjugated CD4 (RM4-5), GL-7 (Ly-77); and secondary streptavidin-APC, streptavidin-PE, or streptavidin-PE-Cy5.5 mAbs (all BD or eBioscience). Intracellular Foxp3 (FJK-16s, FITC-, and APC-conjugated) staining was performed using the Foxp3 staining kit (eBioscience). Samples were analyzed on a FACSCanto II (BD) with FlowJo software (Tree Star). FACS sorting was performed with the FACS Aria cell sorter (BD).

Immunofluorescence and immunohistochemistry. For confocal microscopy, FACS-sorted cells were harvested on slides using cytospin. Cells were fixed and permeabilized with the Foxp3 staining kit (eBioscience). For tissue samples, formalin-fixed paraffin-embedded specimens were prepared (Vaeth et al., 2012). Immunohistochemical reactions were prepared using heat-induced antigen retrieval performed under pressure in citrate-buffer (pH 6.0; Sigma-Aldrich). The following primary antibodies were used: rabbit anti-NFAT1 (Sigma-Aldrich), mouse anti-NFAT2 (7A6; BD), rabbit anti-NFAT2/α (IG-457; immunoGlobe), mouse anti-NFAT4 (F-1; Santa Cruz Biotechnology, Inc.), mouse anti-CD3ε (PS1; Leica), PNA-biotin (Vector Laboratories), rabbit anti-Ig (Dako), and rat anti-Foxp3 (FJK-16s, eBioscience). Secondary staining was performed using the following Abs: anti–rabbit Alexa Fluor 647, anti–mouse Alexa Fluor 488, and anti–rat Alexa Fluor 555 (all from Molecular Probes); anti–IgM-Cy5 (Jackson ImmunoResearch Laboratories); and streptavidin-Alexa Fluor 488 (Invitrogen). Slides were mounted with Fluoromount-G (SouthernBiotech) containing DAPI. Images were taken with a confocal microscope (TCS SP2 equipment, objective lens; HeX PL APO, 40×/1.25-0.75; Leica) and LCS software (Leica). For statistics, >30 cells from at least 2 independent experiments were counted and mean fluorescence intensity per cell (MFI) was calculated. For immunohistochemistry, anti–rabbit HRP (Dianova), anti–rat HRP (Abcam), and Neutravidin HRP (Dianova) were used as secondary Abs. Hematoxylin and eosin staining and PAS staining were performed as previously described (Vaeth et al., 2012).

Real-time PCR. RNA was extracted using RNeasy Micro kit (QIAGEN) followed by cDNA synthesis with the iScript II kit (Bio-Rad Laboratories). Real-time qRT-PCR was performed with an ABI Prism 7700 detection system using following primers: *Nfat2*, 5′-GATCCGAAGCTCGTATGGAC-3′ plus 5′-AGTCTCTTTCCCCGACATCA-3′; *Nfat1*, 5′-TCATAGGAGCCCGACTGATTG-3′ plus 5′-CCATTCCCATCTGCAGCAT-3′; *Nfat4*, 5′-GCCTCCATTGACAGAGCAACT-3′ plus 5′-CACATCCCACAGCCCAGTG-3′; *Nfat2 P1*, 5′-CGGGAGCGGAGAAACTTTGC-3′ plus 5′-CAGGGTCGAGGTGACACTAG-3′; *Nfat2 P2*, 5′-AGGACCCGGAGTTCGACTTC-3′ plus 5′-CAGGGTCGAGGTGACACTAG-3′; *Foxp3*, 5′-GGCCCTTCTCCAGGACAGA-3′ plus 5′-GCTGATCATGGCTGGGTTGT-3′; *Bcl6*, 5′-GATACAGCTGTCAGCCGGG-3′ plus 5′-AGTTTCTAGGAAAGGCCGGA-3′; *Prdm1*, 5′-TAGACTTCACCGATGAGGGG-3′ plus 5′-GTATGCTGCCAACAACAGCA-3′; *Cxcr5*, 5′-TCCTGTAGGGGAATCTCCGT-3′ plus 5′-ACTAACCCTGGACATGGGC-3′; *Hprt*, 5′-AGCCTAAGATGAGCGCAAGT-3′ plus 5′-TTACTAGGCAGATGGCCACA-3′.

Published March 3, 2014

Gene expression analysis. $CD4^+$ T cells from day 7 KLH-immunized WT and *Nfat2*$^{fl/fl}$ x *Cd4cre* mice were negatively enriched (Miltenyi Biotec) followed by FACS-sorting of $CXCR5^-ICOS^-$ T_{naiv}, $CXCR5^-ICOS^{hi}$ T_{act}, and $CXCR5^{hi}ICOS^{hi}$ T_{FH} cells to >95% purity. RNA was extracted using the RNeasy Mini kit (QIAGEN). Biotin-labeled aRNA was prepared with the GeneChip 3′ IVT Express kit and hybridized to GeneChip mouse genome 430 2.0 arrays (Affymetrix) according to the manufacturer's protocol. The trimmed mean signals of the probe arrays were scaled to a target value of 500 and expression values determined using the Affymetrix GeneChip Operating Software (GCOS). Data were analyzed using GeneSpring GX 12.0 software (Agilent Technologies) for significant changes in gene expression between mutant and control samples using the *t* test or 2-way ANOVA, and resulting P values were corrected for multiple testing using the Benjamini-Hochberg method. The original microarray data can be found in the ArrayExpress database under the accession no. E-MEXP-3820 (https://www.ebi.ac.uk/arrayexpress/experiments/E-MEXP-3820/).

ChIP. ChIP-IT Express kit (Active Motif) was used according to the manufacturer's instructions, except enzymatic shearing followed by additional 25-min sonication. After precipitating, the following Abs (5 µg) were used: anti-NFAT2 (7A6; BD) and anti–acetyl-histone H3 (Active Motif). Quantification of DNA binding was performed by (real-time) PCR using the following primers: *Cxcr5* distal, 5′-CTAGTATTCTTAGGGTTCTTCC-3′ plus 5′-GGGCACTTGATCAACCTGTG-3′; *Cxcr5* middle, 5′-GGCTCGCCTGGGACTGAG-3′ plus 5′-GGGGCTAAGAAAAGAGTACTC-3′; Cxcr5 proximal, 5′-ACTGACTCTGTGGGGGGAG-3′ plus 5′-CTTGCCTCTCGACTCATCTC-3′.

Transwell assay. 5×10^5 $CD4^+$ T cells from day 7 KLH-immunized WT and *Nfat2*$^{fl/fl}$ *x Cd4cre* mice were set in 100 µl complete RPMI without FCS. The cells were placed in the upper transwell (Costar; polycarbonate, pore size 5 µm, 6.5 diam) with the lower transwell containing 600 µl complete RPMI (without FCS) with various concentrations of CXCL13 (R&D Systems) or PBS as control. After 5 h of incubation, cells from the lower well were harvested, stained for flow cytometry (CD4 plus Foxp3), and collected in 150 µl FACS buffer. Transwell cell numbers and T cell phenotype were assessed using a FACS Canto II cytometer (BD; 100 µl/min flow speed for 30 s).

ELISA. For determination of NP-specific Ab levels in sera from 10 d NP-(27)-KLH–immunized mice (Bhattacharyya et al., 2011), samples were applied in threefold serial dilutions starting from a 1:20 initial dilution, and their concentration was quantified against a reference serum. For detection of anti-dsDNA Abs in sera of chromatin-immunized mice, blood samples were taken 8 wk after first immunization. Total Ig or IgG anti-dsDNA serum titers were analyzed with a quantitative mouse anti-dsDNA Ig (total A+G+M) ELISA kit (Alpha Diagnostic International) according to the manufacturer's instructions.

EMSA. Nuclear extracts from murine T_{conv} and $Foxp3^+$ T_{reg} cells as well as whole cellular extracts from transiently transfected HEK 293T cells were prepared using the ProteoJET kit (Thermo Fisher Scientific). EMSA was performed, as previously described (Schmidt et al., 2008), with the following probes: *Cxcr5-N1*, 5′-GAAAAGACTCAGTGGAAAAAAAAAAAAA-AAG-3′; *Cxcr5-N1mut*, 5′-GAAAAGACTCAGTAAAAAAAAAAAAA-AAAG-3′; *Cxcr5-N2*, 5′-GGGGGGAGTTTCCCTTTTTCTTAAA-3′; *Cxcr5-N3*, 5′-GGGATGGTTGGTCACCCTAGTGATAAGGAAAGTG-3′; *Cxcr5-N4*, 5′-GGACTGAGGGGTTTCCCAGGACAGGGGACTT-3′; *IL2-Pubd*, 5′-CCCCAAAGAGGAAAATTTGTTT-3′. The mutations are underlined. For super-shifting anti-NFAT2 (7A6; BD) and anti-NFAT1 (Cell Signaling Technology) Abs were used.

Plasmids. HA-Nc1-RSD, HA-NFAT2/C (HA-NFATc1/C), and Blimp-1-Flag have been described (Klein-Hessling et al., 2003; Schmidt et al., 2008; Nayak et al., 2009). The *Cxcr5* promoter (Wolf et al., 1998) elements of murine *Cxcr5* (exact sequences in Fig. S1) were cloned into NheI–NcoI matching *Cxcr5*-ATG with luciferase ATG and HS1 or HS2 into the SalI-site of pGL3-Basic (Invitrogen).

Reporter gene assays. HEK 293T cells, Jurkat T, or EL-4 cells were transiently transfected with different *Cxcr5* promoter luciferase-reporter constructs alone or in combination with a plasmid encoding for NFAT2/C using calcium phosphate, Superfect reagent (Invitrogen), and DEAE dextran, respectively. 36 h after transfection, luciferase activity was measured from the cells that were left untreated, treated with T/I or T/I plus CsA overnight and relative light units were corrected for the transfection efficacy due to total protein concentrations. Normalized mean values of at least three independent experiments are depicted in relative light units as fold activation over empty vector control.

Lentiviral transduction of primary nT_{reg} cells and adoptive transfer experiments. Primary $CD4^+CD25^+$ nT_{reg} cells from WT and *Nfat2*$^{fl/fl}$ *x Cd4cre* mice were activated with anti-CD3/CD28 beads (Invitrogen) for 3 d in presence of 50 U/ml IL-2. Beads were removed and 5×10^6 nT_{reg} cells were collected and resuspended in 1 ml fresh RPMI medium containing 8 µg/ml polybrene (Santa Cruz Biotechnology) and 50 U/ml lL-2 (PeproTech). After 30 min, cells were centrifuged and the supernatant was mostly removed. Cell pellets were resuspended in 0.25 ml/2.5×10^6 IFU ready-made lentiviral solution (*gfp* or *Cxcr5-gfp* [pLenti-EF1a(mCXCR5)-Rsv(GFP-Puro)]; Amsbio) and transduction was performed by spin infection (1,800 rpm for 90 min at 32°C). Then cells were diluted in 2 ml RPMI medium containing 50 U/ml lL-2 (PeproTech) and incubated for additional 4 h at 37°C. In the meantime, $CD4^+CD25^-CD62L^{hi}$ T cells and B cells were isolated from WT mice using the naive T cell isolation kit and the untouched B cell isolation kit, respectively (Miltenyi Biotec). nT_{reg} cells were washed twice and 4×10^5 transduced WT or NFAT-deficient nT_{reg}cells along with 5×10^6 B cells and 2×10^6 naive T cells were adoptively transferred i.p. into *Rag1*$^{-/-}$ mice. After 14 d, mice were immunized with 100 µg NP-KLH and analyzed on day 21.

Statistical analysis. Results were compared with Prism software (GraphPad) using two-tailed paired or unpaired Student's *t* test and two-way ANOVA. Differences with p-values of <0.05 are considered significant: *, $P < 0.05$; **, $P < 0.005$; ***, $P < 0.001$.

Online supplemental material. Fig. S1 shows a scheme of the *Cxcr5* promoter region. Online supplemental material is available at http://www.jem.org/cgi/content/full/jem.20130604/DC1.

We are indebted to Anjana Rao for providing *Nfat2* floxed mice as well as Laurie H. Glimcher for *Nfat1*$^{-/-}$ and *Nfat1*$^{-/-}$ *x Nfat4*$^{-/-}$, Kajsa Wing and Shimon Sakaguchi for *Foxp3-IRES-cre*$^+$, and Tim Sparwasser for *Foxp3*$^{DTR\text{-}eGFP}$ mice. Mice were kept at the Center for Molecular Medicine – ZEMM of the University of Wuerzburg. Appreciation is expressed to Miriam Eckstein, Andra Eisenmann, Ralf Kielenbeck, Doris Michel, Andrea Peters, and Ilona Pietrowski for excellent technical support.

This work was made possible by funding from the Fritz Thyssen Stiftung/Az.10.13.2.215 (M.V. + F.B.-S.), the German Research Foundation DFG: Priority Program SPP1365 (M.V. + F.B.-S.), Collaborative Research Centre/Transregio CRC/TR52/A3 (F.B.-S.), CRC/TR52/B8 (M.L. & G.M.), and CRC/TR52/C5 (E.S.), and Clinical Research Unit CRU216 (I.B.) as well as from the Federal Ministry for Education and Research: IZKF/A-167 in Würzburg, Germany (L.D. + F.B.-S.) and the Wilhelm Sander-Stiftung/2012.047.1 (M.V. + F.B.-S.).

The authors have no competing financial interests.

Submitted: 22 March 2013
Accepted: 3 February 2014

REFERENCES

Alexander, C.M., L.T. Tygrett, A.W. Boyden, K.L. Wolniak, K.L. Legge, and T.J. Waldschmidt. 2011. T regulatory cells participate in the control of germinal centre reactions. *Immunology*. 133:452–468. http://dx.doi.org/10.1111/j.1365-2567.2011.03456.x

Ballesteros-Tato, A., B. León, B.A. Graf, A. Moquin, P.S. Adams, F.E. Lund, and T.D. Randall. 2012. Interleukin-2 inhibits germinal center formation by limiting T follicular helper cell differentiation. *Immunity*. 36:847–856. http://dx.doi.org/10.1016/j.immuni.2012.02.012

Published March 3, 2014

Barnden, M.J., J. Allison, W.R. Heath, and F.R. Carbone. 1998. Defective TCR expression in transgenic mice constructed using cDNA-based alpha- and beta-chain genes under the control of heterologous regulatory elements. *Immunol. Cell Biol.* 76:34–40. http://dx.doi.org/10.1046/j.1440-1711.1998.00709.x

Bauquet, A.T., H. Jin, A.M. Paterson, M. Mitsdoerffer, I.C. Ho, A.H. Sharpe, and V.K. Kuchroo. 2009. The costimulatory molecule ICOS regulates the expression of c-Maf and IL-21 in the development of follicular T helper cells and TH-17 cells. *Nat. Immunol.* 10:167–175. http://dx.doi.org/10.1038/ni.1690

Bhattacharyya, S., J. Deb, A.K. Patra, D.A. Thuy Pham, W. Chen, M. Vaeth, F. Berberich-Siebelt, S. Klein-Hessling, E.D. Lamperti, K. Reifenberg, et al. 2011. NFATc1 affects mouse splenic B cell function by controlling the calcineurin—NFAT signaling network. *J. Exp. Med.* 208:823–839. http://dx.doi.org/10.1084/jem.20100945

Bodor, J., T. Bopp, M. Vaeth, M. Klein, E. Serfling, T. Hünig, C. Becker, H. Schild, and E. Schmitt. 2012. Cyclic AMP underpins suppression by regulatory T cells. *Eur. J. Immunol.* 42:1375–1384. http://dx.doi.org/10.1002/eji.201141578

Bollig, N., A. Brüstle, K. Kellner, W. Ackermann, E. Abass, H. Raifer, B. Camara, C. Brendel, G. Giel, E. Bothur, et al. 2012. Transcription factor IRF4 determines germinal center formation through follicular T-helper cell differentiation. *Proc. Natl. Acad. Sci. USA.* 109:8664–8669. http://dx.doi.org/10.1073/pnas.1205834109

Bonelli, M., A. Savitskaya, K. von Dalwigk, C.W. Steiner, D. Aletaha, J.S. Smolen, and C. Scheinecker. 2008. Quantitative and qualitative deficiencies of regulatory T cells in patients with systemic lupus erythematosus (SLE). *Int. Immunol.* 20:861–868. http://dx.doi.org/10.1093/intimm/dxn044

Bonelli, M., J.S. Smolen, and C. Scheinecker. 2010. Treg and lupus. *Ann. Rheum. Dis.* 69(Suppl 1):i65–i66. http://dx.doi.org/10.1136/ard.2009.117135

Bopp, T., C. Becker, M. Klein, S. Klein-Hessling, A. Palmetshofer, E. Serfling, V. Heib, M. Becker, J. Kubach, S. Schmitt, et al. 2007. Cyclic adenosine monophosphate is a key component of regulatory T cell-mediated suppression. *J. Exp. Med.* 204:1303–1310. http://dx.doi.org/10.1084/jem.20062129

Chaudhry, A., D. Rudra, P. Treuting, R.M. Samstein, Y. Liang, A. Kas, and A.Y. Rudensky. 2009. CD4+ regulatory T cells control TH17 responses in a Stat3-dependent manner. *Science.* 326:986–991. http://dx.doi.org/10.1126/science.1172702

Chtanova, T., S.G. Tangye, R. Newton, N. Frank, M.R. Hodge, M.S. Rolph, and C.R. Mackay. 2004. T follicular helper cells express a distinctive transcriptional profile, reflecting their role as non-Th1/Th2 effector cells that provide help for B cells. *J. Immunol.* 173:68–78.

Chung, Y., S. Tanaka, F. Chu, R.I. Nurieva, G.J. Martinez, S. Rawal, Y.H. Wang, H. Lim, J.M. Reynolds, X.H. Zhou, et al. 2011. Follicular regulatory T cells expressing Foxp3 and Bcl-6 suppress germinal center reactions. *Nat. Med.* 17:983–988. http://dx.doi.org/10.1038/nm.2426

Chuvpilo, S., E. Jankevics, D. Tyrsin, A. Akimzhanov, D. Moroz, M.K. Jha, J. Schulze-Luehrmann, B. Santner-Nanan, E. Feoktistova, T. König, et al. 2002. Autoregulation of NFATc1/A expression facilitates effector T cells to escape from rapid apoptosis. *Immunity.* 16:881–895. http://dx.doi.org/10.1016/S1074-7613(02)00329-1

Cretney, E., A. Xin, W. Shi, M. Minnich, F. Masson, M. Miasari, G.T. Belz, G.K. Smyth, M. Busslinger, S.L. Nutt, and A. Kallies. 2011. The transcription factors Blimp-1 and IRF4 jointly control the differentiation and function of effector regulatory T cells. *Nat. Immunol.* 12:304–311. http://dx.doi.org/10.1038/ni.2006

Cretney, E., A. Kallies, and S.L. Nutt. 2013. Differentiation and function of Foxp3(+) effector regulatory T cells. *Trends Immunol.* 34:74–80. http://dx.doi.org/10.1016/j.it.2012.11.002

Crotty, S. 2011. Follicular helper CD4 T cells (TFH). *Annu. Rev. Immunol.* 29:621–663. http://dx.doi.org/10.1146/annurev-immunol-031210-101400

Farrow, M.A., E.Y. Kim, S.M. Wolinsky, and A.M. Sheehy. 2011. NFAT and IRF proteins regulate transcription of the anti-HIV gene, APOBEC3G. *J. Biol. Chem.* 286:2567–2577. http://dx.doi.org/10.1074/jbc.M110.154377

Hill, J.A., M. Feuerer, K. Tash, S. Haxhinasto, J. Perez, R. Melamed, D. Mathis, and C. Benoist. 2007. Foxp3 transcription-factor-dependent and -independent regulation of the regulatory T cell transcriptional signature. *Immunity.* 27:786–800. http://dx.doi.org/10.1016/j.immuni.2007.09.010

Ho, I.C., M.R. Hodge, J.W. Rooney, and L.H. Glimcher. 1996. The proto-oncogene c-maf is responsible for tissue-specific expression of interleukin-4. *Cell.* 85:973–983. http://dx.doi.org/10.1016/S0092-8674(00)81299-4

Hock, M., M. Vaeth, R. Rudolf, A.K. Patra, D.A.T. Pham, K. Muhammad, T. Pusch, T. Bopp, E. Schmitt, R. Rost, et al. 2013. NFATc1 induction in peripheral T and B lymphocytes. *J. Immunol.* 190:2345–2353.

Ise, W., M. Kohyama, B.U. Schraml, T. Zhang, B. Schwer, U. Basu, F.W. Alt, J. Tang, E.M. Oltz, T.L. Murphy, and K.M. Murphy. 2011. The transcription factor BATF controls the global regulators of class-switch recombination in both B cells and T cells. *Nat. Immunol.* 12:536–543.

Jasinski, J.M., L. Yu, M. Nakayama, M.M. Li, M.A. Lipes, G.S. Eisenbarth, and E. Liu. 2006. Transgenic insulin (B:9-23) T-cell receptor mice develop autoimmune diabetes dependent upon RAG genotype, H-2g7 homozygosity, and insulin 2 gene knockout. *Diabetes.* 55:1978–1984. http://dx.doi.org/10.2337/db06-0058

Johnston, R.J., A.C. Poholek, D. DiToro, I. Yusuf, D. Eto, B. Barnett, A.L. Dent, J. Craft, and S. Crotty. 2009. Bcl6 and Blimp-1 are reciprocal and antagonistic regulators of T follicular helper cell differentiation. *Science.* 325:1006–1010. http://dx.doi.org/10.1126/science.1175870

Johnston, R.J., Y.S. Choi, J.A. Diamond, J.A. Yang, and S. Crotty. 2012. STAT5 is a potent negative regulator of TFH cell differentiation. *J. Exp. Med.* 209:243–250. http://dx.doi.org/10.1084/jem.20111174

Josefowicz, S.Z., L.F. Lu, and A.Y. Rudensky. 2012. Regulatory T cells: mechanisms of differentiation and function. *Annu. Rev. Immunol.* 30:531–564. http://dx.doi.org/10.1146/annurev.immunol.25.022106.141623

Klein-Hessling, S., M.K. Jha, B. Santner-Nanan, F. Berberich-Siebelt, T. Baumruker, A. Schimpl, and E. Serfling. 2003. Protein kinase A regulates GATA-3-dependent activation of IL-5 gene expression in Th2 cells. *J. Immunol.* 170:2956–2961.

Klein-Hessling, S., T. Bopp, M.K. Jha, A. Schmidt, S. Miyatake, E. Schmitt, and E. Serfling. 2008. Cyclic AMP-induced chromatin changes support the NFATc-mediated recruitment of GATA-3 to the interleukin 5 promoter. *J. Biol. Chem.* 283:31030–31037. http://dx.doi.org/10.1074/jbc.M805929200

Koch, M.A., G. Tucker-Heard, N.R. Perdue, J.R. Killebrew, K.B. Urdahl, and D.J. Campbell. 2009. The transcription factor T-bet controls regulatory T cell homeostasis and function during type 1 inflammation. *Nat. Immunol.* 10:595–602. http://dx.doi.org/10.1038/ni.1731

Kroenke, M.A., D. Eto, M. Locci, M. Cho, T. Davidson, E.K. Haddad, and S. Crotty. 2012. Bcl6 and Maf cooperate to instruct human follicular helper CD4 T cell differentiation. *J. Immunol.* 188:3734–3744. http://dx.doi.org/10.4049/jimmunol.1103246

Kuo, T.C., and K.L. Calame. 2004. B lymphocyte-induced maturation protein (Blimp)-1, IFN regulatory factor (IRF)-1, and IRF-2 can bind to the same regulatory sites. *J. Immunol.* 173:5556–5563.

Kusam, S., L.M. Toney, H. Sato, and A.L. Dent. 2003. Inhibition of Th2 differentiation and GATA-3 expression by BCL-6. *J. Immunol.* 170:2435–2441.

Kwon, H., D. Thierry-Mieg, J. Thierry-Mieg, H.P. Kim, J. Oh, C. Tunyaplin, S. Carotta, C.E. Donovan, M.L. Goldman, P. Tailor, et al. 2009. Analysis of interleukin-21-induced Prdm1 gene regulation reveals functional cooperation of STAT3 and IRF4 transcription factors. *Immunity.* 31:941–952. http://dx.doi.org/10.1016/j.immuni.2009.10.008

Lahl, K., C. Loddenkemper, C. Drouin, J. Freyer, J. Arnason, G. Eberl, A. Hamann, H. Wagner, J. Huehn, and T. Sparwasser. 2007. Selective depletion of Foxp3+ regulatory T cells induces a scurfy-like disease. *J. Exp. Med.* 204:57–63. http://dx.doi.org/10.1084/jem.20061852

Lee, P.P., D.R. Fitzpatrick, C. Beard, H.K. Jessup, S. Lehar, K.W. Makar, M. Pérez-Melgosa, M.T. Sweetser, M.S. Schlissel, S. Nguyen, et al. 2001. A critical role for Dnmt1 and DNA methylation in T cell development, function, and survival. *Immunity.* 15:763–774. http://dx.doi.org/10.1016/S1074-7613(01)00227-8

Li, H., Y.Y. Zhang, Y.N. Sun, X.Y. Huang, Y.F. Jia, and D. Li. 2004. Induction of systemic lupus erythematosus syndrome in BALB/c mice by immunization with active chromatin. *Acta Pharmacol. Sin.* 25:807–811.

Lim, H.W., P. Hillsamer, A.H. Banham, and C.H. Kim. 2005. Cutting edge: direct suppression of B cells by CD4+ CD25+ regulatory T cells. *J. Immunol.* 175:4180–4183.

Linterman, M.A., W. Pierson, S.K. Lee, A. Kallies, S. Kawamoto, T.F. Rayner, M. Srivastava, D.P. Divekar, L. Beaton, J.J. Hogan, et al. 2011. Foxp3+ follicular regulatory T cells control the germinal center response. *Nat. Med.* 17:975–982. http://dx.doi.org/10.1038/nm.2425

Liu, X., X. Yan, B. Zhong, R.I. Nurieva, A. Wang, X. Wang, N. Martin-Orozco, Y. Wang, S.H. Chang, E. Esplugues, et al. 2012. Bcl6 expression specifies the T follicular helper cell program in vivo. *J. Exp. Med.* 209:1841–1852: S1–S24. http://dx.doi.org/10.1084/jem.20120219

Ma, C.S., E.K. Deenick, M. Batten, and S.G. Tangye. 2012. The origins, function, and regulation of T follicular helper cells. *J. Exp. Med.* 209:1241–1253. http://dx.doi.org/10.1084/jem.20120994

McCaffrey, P.G., P.K. Kim, V.E. Valge-Archer, R. Sen, and A. Rao. 1994. Cyclosporin A sensitivity of the NF-kappa B site of the IL2R alpha promoter in untransformed murine T cells. *Nucleic Acids Res.* 22:2134–2142. http://dx.doi.org/10.1093/nar/22.11.2134

Müller, M.R., and A. Rao. 2010. NFAT, immunity and cancer: a transcription factor comes of age. *Nat. Rev. Immunol.* 10:645–656. http://dx.doi.org/10.1038/nri2818

Nayak, A., J. Glöckner-Pagel, M. Vaeth, J.E. Schumann, M. Buttmann, T. Bopp, E. Schmitt, E. Serfling, and F. Berberich-Siebelt. 2009. Sumoylation of the transcription factor NFATc1 leads to its subnuclear relocalization and interleukin-2 repression by histone deacetylase. *J. Biol. Chem.* 284:10935–10946. http://dx.doi.org/10.1074/jbc.M900465200

Oestreich, K.J., S.E. Mohn, and A.S. Weinmann. 2012. Molecular mechanisms that control the expression and activity of Bcl-6 in TH1 cells to regulate flexibility with a TFH-like gene profile. *Nat. Immunol.* 13:405–411. http://dx.doi.org/10.1038/ni.2242

Peng, S.L., A.J. Gerth, A.M. Ranger, and L.H. Glimcher. 2001. NFATc1 and NFATc2 together control both T and B cell activation and differentiation. *Immunity.* 14:13–20. http://dx.doi.org/10.1016/S1074-7613(01)00085-1

Qiao, B., J. Wu, Y.W. Chu, Y. Wang, D.P. Wang, H.S. Wu, and S.D. Xiong. 2005. Induction of systemic lupus erythematosus-like syndrome in syngeneic mice by immunization with activated lymphocyte-derived DNA. *Rheumatology (Oxford).* 44:1108–1114. http://dx.doi.org/10.1093/rheumatology/keh656

Ranger, A.M., M.R. Hodge, E.M. Gravallese, M. Oukka, L. Davidson, F.W. Alt, F.C. de la Brousse, T. Hoey, M. Grusby, and L.H. Glimcher. 1998. Delayed lymphoid repopulation with defects in IL-4-driven responses produced by inactivation of NF-ATc. *Immunity.* 8:125–134. http://dx.doi.org/10.1016/S1074-7613(00)80465-3

Rasheed, A.U., H.P. Rahn, F. Sallusto, M. Lipp, and G. Müller. 2006. Follicular B helper T cell activity is confined to CXCR5(hi)ICOS(hi) CD4 T cells and is independent of CD57 expression. *Eur. J. Immunol.* 36:1892–1903. http://dx.doi.org/10.1002/eji.200636136

Rengarajan, J., K.A. Mowen, K.D. McBride, E.D. Smith, H. Singh, and L.H. Glimcher. 2002a. Interferon regulatory factor 4 (IRF4) interacts with NFATc2 to modulate interleukin 4 gene expression. *J. Exp. Med.* 195:1003–1012. http://dx.doi.org/10.1084/jem.20011128

Rengarajan, J., B. Tang, and L.H. Glimcher. 2002b. NFATc2 and NFATc3 regulate T(H)2 differentiation and modulate TCR-responsiveness of naïve T(H)cells. *Nat. Immunol.* 3:48–54. http://dx.doi.org/10.1038/ni744

Sage, P.T., L.M. Francisco, C.V. Carman, and A.H. Sharpe. 2013. The receptor PD-1 controls follicular regulatory T cells in the lymph nodes and blood. *Nat. Immunol.* 14:152–161. http://dx.doi.org/10.1038/ni.2496

Sakaguchi, S., T. Yamaguchi, T. Nomura, and M. Ono. 2008. Regulatory T cells and immune tolerance. *Cell.* 133:775–787. http://dx.doi.org/10.1016/j.cell.2008.05.009

Schmidt, D., A. Nayak, J.E. Schumann, A. Schimpl, I. Berberich, and F. Berberich-Siebelt. 2008. Blimp-1Deltaexon7: a naturally occurring Blimp-1 deletion mutant with auto-regulatory potential. *Exp. Cell Res.* 314:3614–3627. http://dx.doi.org/10.1016/j.yexcr.2008.09.008

Serfling, E., F. Berberich-Siebelt, S. Chuvpilo, E. Jankevics, S. Klein-Hessling, T. Twardzik, and A. Avots. 2000. The role of NF-AT transcription factors in T cell activation and differentiation. *Biochim. Biophys. Acta.* 1498:1–18. http://dx.doi.org/10.1016/S0167-4889(00)00082-3

Serfling, E., A. Avots, S. Klein-Hessling, R. Rudolf, M. Vaeth, and F. Berberich-Siebelt. 2012. NFATc1/αA: The other Face of NFAT Factors in Lymphocytes. *Cell Commun. Signal.* 10:16. http://dx.doi.org/10.1186/1478-811X-10-16

Shaffer, A.L., K.I. Lin, T.C. Kuo, X. Yu, E.M. Hurt, A. Rosenwald, J.M. Giltnane, L. Yang, H. Zhao, K. Calame, and L.M. Staudt. 2002. Blimp-1 orchestrates plasma cell differentiation by extinguishing the mature B cell gene expression program. *Immunity.* 17:51–62. http://dx.doi.org/10.1016/S1074-7613(02)00335-7

Simpson, N., P.A. Gatenby, A. Wilson, S. Malik, D.A. Fulcher, S.G. Tangye, H. Manku, T.J. Vyse, G. Roncador, G.A. Huttley, et al. 2010. Expansion of circulating T cells resembling follicular helper T cells is a fixed phenotype that identifies a subset of severe systemic lupus erythematosus. *Arthritis Rheum.* 62:234–244. http://dx.doi.org/10.1002/art.25032

Vaeth, M., T. Gogishvili, T. Bopp, M. Klein, F. Berberich-Siebelt, S. Gattenloehner, A. Avots, T. Sparwasser, N. Grebe, E. Schmitt, et al. 2011. Regulatory T cells facilitate the nuclear accumulation of inducible cAMP early repressor (ICER) and suppress nuclear factor of activated T cell c1 (NFATc1). *Proc. Natl. Acad. Sci. USA.* 108:2480–2485. http://dx.doi.org/10.1073/pnas.1009463108

Vaeth, M., U. Schliesser, G. Müller, S. Reissig, K. Satoh, A. Tuettenberg, H. Jonuleit, A. Waisman, M.R. Müller, E. Serfling, et al. 2012. Dependence on nuclear factor of activated T-cells (NFAT) levels discriminates conventional T cells from Foxp3+ regulatory T cells. *Proc. Natl. Acad. Sci. USA.* 109:16258–16263. http://dx.doi.org/10.1073/pnas.1203870109

Valencia, X., C. Yarboro, G. Illei, and P.E. Lipsky. 2007. Deficient CD4+CD25high T regulatory cell function in patients with active systemic lupus erythematosus. *J. Immunol.* 178:2579–2588.

Wang, J., and A. Yen. 2004. A novel retinoic acid-responsive element regulates retinoic acid-induced BLR1 expression. *Mol. Cell. Biol.* 24:2423–2443. http://dx.doi.org/10.1128/MCB.24.6.2423-2443.2004

Wing, K., Y. Onishi, P. Prieto-Martin, T. Yamaguchi, M. Miyara, Z. Fehervari, T. Nomura, and S. Sakaguchi. 2008. CTLA-4 control over Foxp3+ regulatory T cell function. *Science.* 322:271–275. http://dx.doi.org/10.1126/science.1160062

Wolf, I., V. Pevzner, E. Kaiser, G. Bernhardt, E. Claudio, U. Siebenlist, R. Förster, and M. Lipp. 1998. Downstream activation of a TATA-less promoter by Oct-2, Bob1, and NF-kappaB directs expression of the homing receptor BLR1 to mature B cells. *J. Biol. Chem.* 273:28831–28836. http://dx.doi.org/10.1074/jbc.273.44.28831

Wollenberg, I., A. Agua-Doce, A. Hernández, C. Almeida, V.G. Oliveira, J. Faro, and L. Graca. 2011. Regulation of the germinal center reaction by Foxp3+ follicular regulatory T cells. *J. Immunol.* 187:4553–4560. http://dx.doi.org/10.4049/jimmunol.1101328

Yu, D., S. Rao, L.M. Tsai, S.K. Lee, Y. He, E.L. Sutcliffe, M. Srivastava, M. Linterman, L. Zheng, N. Simpson, et al. 2009. The transcriptional repressor Bcl-6 directs T follicular helper cell lineage commitment. *Immunity.* 31:457–468. http://dx.doi.org/10.1016/j.immuni.2009.07.002

Zheng, Y., S.Z. Josefowicz, A. Kas, T.T. Chu, M.A. Gavin, and A.Y. Rudensky. 2007. Genome-wide analysis of Foxp3 target genes in developing and mature regulatory T cells. *Nature.* 445:936–940. http://dx.doi.org/10.1038/nature05563

SUPPLEMENTAL MATERIAL

Vaeth et al., http://www.jem.org/cgi/content/full/jem.20130604/DC1

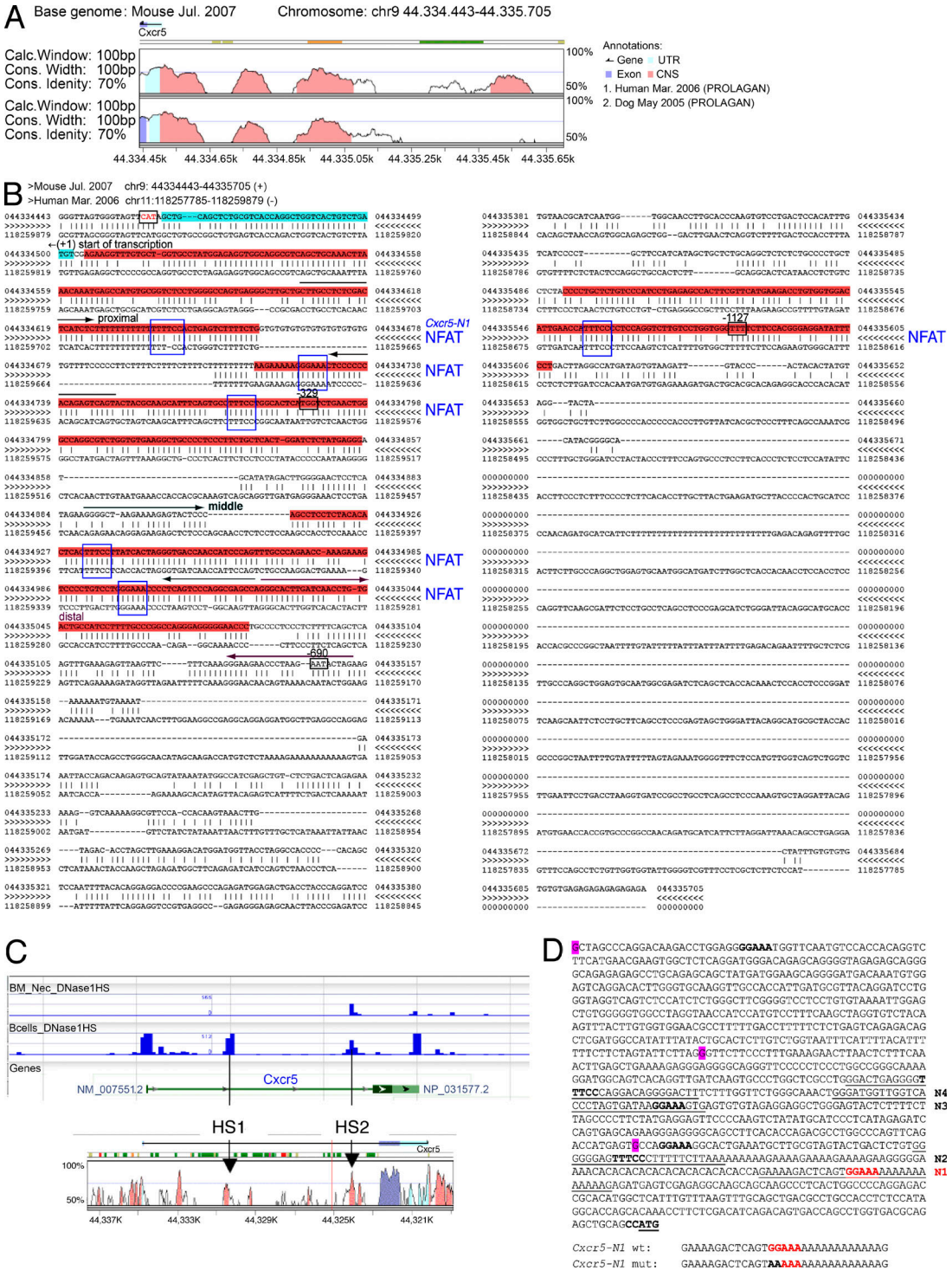

Figure S1. Scheme of *Cxcr5* promoter region. (A) Alignment of human and dog *Cxcr5* promoter reveals conserved noncoding sequences (CNS). (B) DNA sequence alignment of murine and human *Cxcr5* promoter shown in A. Potential binding sites of NFAT, constructs used in reporter gene assays, and primers for ChIP experiments are illustrated. (C) Identification of potential regulatory elements (HS2 and HS1) within the *Cxcr5* gene using public DNase I mapping data. (D) Sequence of the *Cxcr5* promoter; starting nucleotides for luciferase constructs in purple, probes used for EMSA underlined and names given at the side. The GG→AA mutation within *Cxcr5-N1* (red) is shown below.